ENERGY HARVESTER DESIGN METHOD TO POWER WIRELESS SENSOR NODES FOR IN PIPE MONITORING APPLICATIONS

FASSAHAT ULLAH QURESHI

JULY 2016

ENERGY HARVESTER DESIGN METHOD TO POWER WIRELESS SENSOR NODES FOR IN PIPE MONITORING APPLICATIONS

SUSTAINABLE ENVIRONMENT AND ENERGY SYSTEMS

MIDDLE EAST TECHNICAL UNIVERSITY,

NORTHERN CYPRUS CAMPUS

BY

FASSAHAT ULLAH QURESHI

IN PARTIAL FULFILLMENT OF THE REQUIREMENTS

FOR

THE DEGREE OF MASTER OF SCIENCE

IN

SUSTAINABLE ENVIRONMENT AND ENERGY SYSTEMS PROGRAM

JULY 2016

Approval of the Board of Graduate Programs

_____

Prof. Dr. M. Tanju MEHMETOĞLU

Chairperson

I certify that this thesis satisfies all the requirements as a thesis for the degree of Master of Science

_____

Assoc. Prof. Dr. Ali Muhtaroğlu

Program Coordinator

This is to certify that we have read this thesis and that in our opinion it is fully adequate, in scope and quality, as a thesis for the degree of Master of Science.

_____

Assoc. Prof. Dr. Ali Muhtaroğlu

Supervisor

Examining Committee Members

Prof. Dr. Kagan Tuncay, Jury Chair	Civil Engineering, METU	_____
Assoc. Prof. Dr. Ali Muhtaroğlu, Jury Member	Electrical and Electronics Engineering, METU NCC	_____
Assoc. Prof. Dr. Murat Fahrioglu, Jury Member	Electrical and Electronics Engineering, METU NCC	_____
Assoc. Prof. Dr. Volkan Esat, Jury Member	Mechanical Engineering, METU NCC	_____
Assoc. Prof. Dr. Tayfun Nesimoglu, Jury Member	Electrical and Electronics Engineering, METU NCC	_____

ETHICAL DECLARATION

I hereby declare that all information in this document has been obtained and presented in accordance with academic rules and ethical conduct. I also declare that, as required by these rules and conduct, I have fully cited and referenced all material and results that are not original to this work.

Name, Last Name: Fassahat Ullah Qureshi

Signature:

ABSTRACT

ENERGY HARVESTER DESIGN METHOD TO POWER WIRELESS SENSOR NODES FOR IN PIPE MONITORING APPLICATIONS

Qureshi, Fassahat Ullah

M.Sc., Sustainable Environment and Energy Systems

Supervisor : Assoc. Prof. Dr. Ali Muhtaroğlu

July 2016, 66 pages

A sensor network, used to monitor water, oil or gas pipelines, consists of a group of wireless sensor nodes (WSN) that are linked using a communication infrastructure. Traditional batteries are commonly used to power sensor nodes, but they have limited lifetime and require regular maintenance. Thus, their utility is limited in locations that are difficult to access, such as underwater pipelines. Therefore, using an energy harvester to power the sensor node becomes a desirable option. A method for near-optimal piezoelectric (PZT) bimorph energy harvester module design with minimum impact on the pipe performance is proposed in this study to enable a self-powered wireless sensor node for in-pipe monitoring. An analytical model is presented as the starting point of this research, which is further validated through finite element simulations using COMSOL software in 2D (two dimensional) environment. Geometry sensitivity analysis and optimization is done through finite element simulations. The boundary conditions of the recently constructed Turkey-Cyprus water pipeline are considered for finite element analysis with a flow velocity of 1.4 m/s. Performance impact analysis is also done in terms of head loss to compare two PZT cantilever energy harvesters attached to I- and D-shaped bluff bodies. Series and parallel arrangements of energy harvesters are compared with respect to generated power, and impact on pipe performance. The geometrically designed energy harvester is able to generate a power of 0.82 mW corresponding to a head loss of 3 mm, which is considered to be a near optimal design. It is concluded from the analysis that 15 PZT cantilevers in parallel arrangement are needed to maintain 4096 bits per second (bps) transmission of 512-Byte data packet once per 5 minutes with the piezoelectric harvester, using an integrated 7.1 J super capacitor that can fit into the bluff body together with the power electronics and acoustic transceiver.

Keywords: Wireless sensor networks, piezoelectric energy harvesting, pipeline, finite element model

ÖZ

BORU İÇİ GÖZETLEME UYGULAMALARINA YÖNELİK KABLOSUZ SENSÖR DÜĞÜMLERİNE GÜÇ SAĞLAYAN ENERJİ ÜRETECİ TASARIM YÖNTEMİ

Qureshi, Fassahat Ullah

Master, Sürdürülebilir Çevre ve Enerji Sistemleri

Tez Yöneticisi : Doç. Dr. Ali Muhtaroğlu

Haziran 2016, 66 sayfa

Su, petrol veya gaz boru hatlarını izlemek için kullanılan sensör ağı, iletişim altyapısı kullanılarak bağlanan bir grup kablosuz sensör düğümünden (KSD) oluşur. Sensör düğümlerine güç sağlamak için kullanılan geleneksel piller sınırlı ömre sahiptir ve düzenli servis gerektirir. Bu sebepten dolayı su altı boru hatları gibi erişilmesi zor yerlerde kullanımları sınırlıdır. Bu zorluklar sensör düğümüne güç sağlamak için enerji üreteci kullanmayı cazip bir seçenek haline getirmektedir. Çalışmanın amacı boru içinde kendi gücünü üreten ve boru performansına en az etkisi olan piezoelektrik (PZT) bimorf enerji üreteci tasarlamaktır. Bu araştırmanın başlangıç noktası olarak analitik bir model sunulmakta daha sonraysa bu model iki boyutlu sonlu elemanlar yöntemiyle COMSOL yazılımı kullanılarak doğrulanmaktadır. Geometri duyarlılık analizi ve optimizasyonu sonlu eleman simülasyonları ile yapılmaktadır. 1.4 m/s akış hızıyla su taşıyan Türkiye-KKTC boru hattı uygulaması sınır koşullarını belirlemek için kullanılmaktadır. Bir ucu I- ve D-şekilli sabit gövdeye tutturulmuş PZT konsol kiriş türü enerji üreteçlerinin performans etkisi basınç kaybı cinsinden karşılaştırılmaktadır. Ayrıca, seri ve paralel enerji üreteç düzenleri üretilen güç ve boru iletim performansına etki bakımlarından kıyaslanmaktadır. Bahsi geçen uygulamada, geometrik tasarımı tamamlanmış enerji üreteci 0.82 mW güç üretimini 3 mm yükseklik eşdeğer kaybı ile sağlayabilmektedir. Analiz sonucunda, paralel olarak yerleştirilmiş 15 PZT kiriş, sabit gövdeye entegre edilmiş 7.1 J depolayabilen süper kondansatör, güç elektroniği ve akustik alıcı-verici kullanarak 512 baytlık bir veri paketinin saniyede 4096 bit (bps) transmisyon hızı ile 5 dakikada bir iletilebileceği belirlenmiştir.

Anahtar Kelimeler: Kablosuz sensör ağları, piezoelektrik enerji üreteci, boru hattı, sonlu elemanlar modeli

To My Wife

ACKNOWLEDGEMENTS

I wish to express my sincere gratitude and appreciation to all people who supported and inspired me to complete this thesis. I would like to specially thank Assoc. Prof. Dr. Ali Muhtaroğlu, my thesis adviser for his continued support, suggestions, criticism and encouragements during my research. I am so much thankful for his help, professionalism and valuable guidance for this research through my entire program of study that I do not have enough words to express my deep and sincere appreciation.

I would also like to utter my gratefulness to my co-advisor Prof. Dr. Kağan Tuncay, for providing me ideas on how to improve my research and which direction to cover. Besides my advisers, I would also like to acknowledge other members of thesis committee Assoc. Prof. Dr. Murat Fahrioğlu, Assoc. Prof. Dr. Volkan Esat and Assoc. Prof. Dr. Tayfun Nesimoğlu, for their valuable guidance and comments during this research. I would like to thank Turkish Water Department engineer who provided me with the data of Turkey Cyprus water pipeline project

Nobody has been more important to me in the completion of this thesis other than the members of my family. Most importantly, I wish to thank my loving wife Sundas Khalid for her continuous inspiration and support for the completion of this thesis. Finally, I must express my profound gratitude to my parents, who are my ultimate role models for providing me with unfailing support and continuous encouragement throughout my years of study and through the process of researching and writing this thesis. This accomplishment would not have been possible without them. Thank you.

TABLE OF CONTENTS

LIST OF FIGURES

LIST OF TABLES

GLOSSARY

AC:	Alternating Current
CFD:	Computational Fluid Dynamics
D:	Dimension of Bluff Body
DC:	Direct Current
FSI:	Fluid Structure Interaction
L:	Length of Cantilever Beam
PVDF:	Poly vinyl di fluoride
pH:	Potential Hydrogen
PZT:	Piezoelectric
Re:	Reynolds Number
RF:	Radio Frequency
Sr:	Strouhal Number
T_{PZTmin}:	Minimum Thickness of PZT cantilever
UW:	Underwater
WSN:	Wireless Sensor Node
Y:	Young's Modulus
η:	Dynamic Viscosity
λ:	Period of the "von Karman's" Vortex Street
σ_{max}:	Ultimate tensile strength of the PZT-Material

CHAPTER 1 - INTRODUCTION

1.1 Motivation

Water, oil and gas are the most important assets of the world as the economic progress of most states depends upon these resources. A common transporter used in distributing these resources is a transmission pipeline. Protecting and monitoring pipelines is very important to avoid waste of resources and reduce operational costs. Various types of sensor networks are used to achieve this goal [1]. Monitoring of underwater pipelines is particularly challenging due to limited access. Many types of sensor networks for monitoring of underwater pipelines are discussed in different studies [2, 3]. Wireless smart sensors in pipes offer a lot of advantages when compared to wired sensors for monitoring water conduits including low cost of placement, maintenance, and safety [4]. Such sensors also often support various data rates and fault positioning features. Energy harvesting for powering in-pipe wireless sensor nodes is an important area of research due to the unavailability of traditional power sources for operating the embedded smart sensor networks for underwater pipeline applications. Various types of energy harvesters such as electromagnetic, piezoelectric and solar energy are discussed in the literature [5]. . A method for near-optimal energy harvester design is proposed in this research to enable a self-powered wireless sensor node for in-pipe monitoring. An implementation based on energy harvesting from water flow is used to operate wireless sensor node, with minimum quantified impact to the native flow rate and/or water pressure.

1.2 Energy Harvesting Background

Different types of energy harvesting techniques are discussed in the literature to generate electric power for operating wireless sensor network nodes. Most of the research has been done on solar energy harvesting [6] which is not applicable to underwater pipelines. Another popular source for energy harvesting is wind energy [7]. Higher elevations are required to achieve at least the cut-in speed of wind turbine so this type of energy harvesting is also ineffective for underwater pipelines. Another possible option is thermoelectric energy harvester which is used to capture energy from the difference of temperature between two resources to produce electrical power but this option cannot be used for underwater pipelines since there is no air available under water. Energy harvesting on the water surface is also another option but it may have certain challenges in terms of security. It has to be connected through wired cables from the underwater pipeline infrastructure to the surface buoys, which may be damaged due to sea currents and ships travelling on the water surface [2]. The potential possible energy harvesting techniques which can be applied to underwater pipelines are discussed in the sections 1.3 and 1.4.

1.3 Electromagnetic Energy Harvesting

Small scale hydro generators scavenge energy from the fluid to operate wireless sensor nodes. According to [8], water flow is utilized to produce electrical energy with the help of Pelton and Propeller turbines. Figure 1.1 shows different types of hydro turbines where (a) and (b) describe the working mechanisms of Pelton and Propeller turbines while (c) and (d) indicate the shape of these turbines.

Energy harvesting from the fluid in distribution water conduits, scavenging thermal energy due to difference of temperature between water and air, and producing energy from the kinetic energy of water are studied comprehensively in [9]. Three different mechanisms using micro turbine were investigated in the study, which are shown in Figure 1.2. Power output is calculated for all mechanisms to determine the most efficient scheme for energy harvesting. Water is directly released from the small pipe to drive the turbine in the first system shown in Figure 1.2 (a). With a water flow rate of 10 liter per second and main pipe radius of 10 cm, about 150 W of power is generated but the system wastes large amount of water continuously. The utilization of the pressure drop after a valve is shown in Figure 1.2 (b) where micro turbine is driven to produce only 0.32 mW power. In the third system presented in Figure 1.2 (c) a pitot pipe to run the micro-turbine is used which generates less than 1 μW. None of the systems is found suitable for energy scavenging in water supply channels.

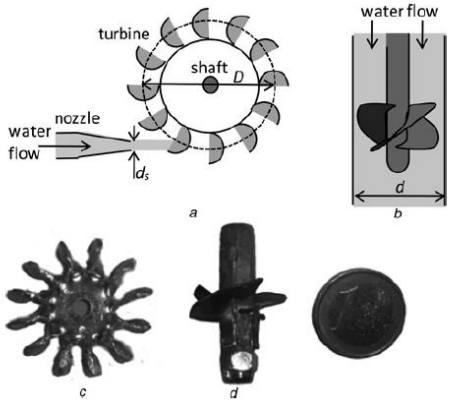

Figure 1.1. Different types of hydro turbines [8].

Energy harvester system component requirements vary depending on which type of system configuration is used. Both wind and water energy systems were investigated

in [10]. In addition, sensor requirements to power wireless sensor node were presented in the same study. However, performance impact of installing an energy harvester on the host was not considered which is one of the main focus points of the present study. Figure 1.3 shows the charge controller circuit that charges a battery which supplies power to a WSN. The node communicates (transmission and reception) at 2.4 GHz where voltages that have a range from 2.1 and 3.6 V can be applied with a current depletion of 40 mA (at 3.3 V). It results in electrical power requirement of only 132 mW if the sensor node is always switched on. This circuit shows that power electronics circuit is also an important component if an energy harvester is to be used instead of battery.

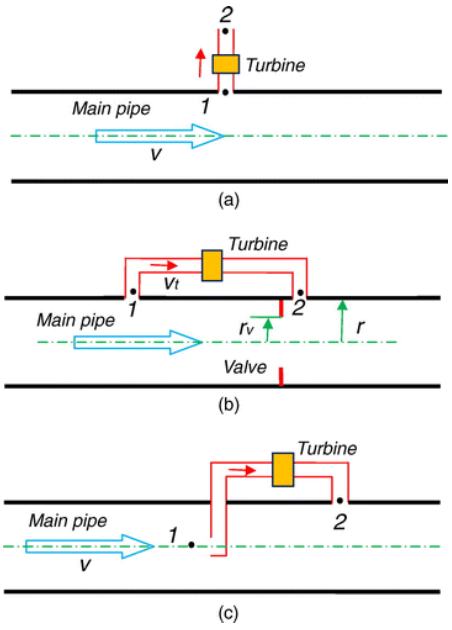

Figure 1.2. Energy harvesting from water flow through three different mechanisms [9].

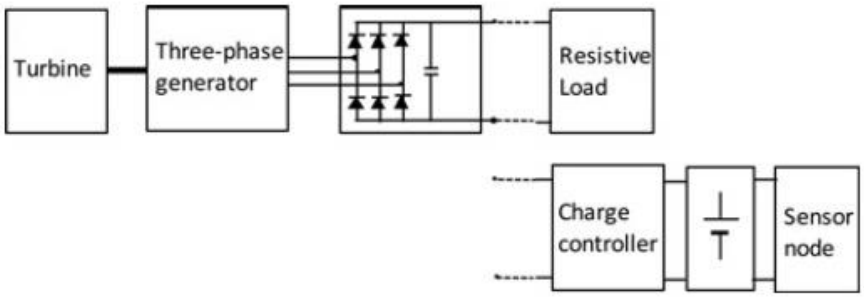

Figure 1.3. Circuit layout for the whole system used in powering the sensor node [11].

Hydropower harvesting for pipeline monitoring is investigated in [12], where new vertical axis turbine is proposed which is designed through Computational Fluid Dynamics (CFD) simulations, and laboratory tests. But, this study did not investigated the head loss if a turbine is installed into the water system. In addition, internal losses of turbines such as rotational and wear losses were not analyzed in the study. Lucid Energy Company [13] developed the vertical axis spherical turbine installed into the large water pipes which is shown in Figure 1.4. Water flows through the hydro turbine, and when it spins electrical power is produced.

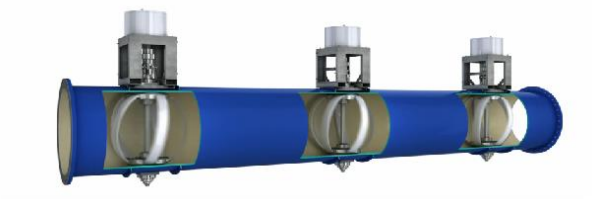

Figure 1.4. Lucid energy lift-type turbines [13].

1.4 Piezoelectric Energy Harvesting

Energy harvesting from continuous vibration caused by fluid flow around piezo-ceramic cantilever beams is studied in [14]. Fluid exerts pressure on the cantilever to produce von Karman's street pattern which in turn generates lift force on the cantilever. Mechanical cantilever vibrates continuously in the direction perpendicular to the flow of the fluid due to variation in the pressure of the fluid. Continuous vibration of the PZT cantilever converts mechanical energy into electrical energy. Another novel hydropower energy harvester is presented in [15]. In order to harvest energy, the kinetic energy of flowing rivers is investigated and two different designs of piezoelectric energy harvesters are studied for the generation of electrical power. The first is a moving flag design which twists periodically in turbulent flow. This fluttering flag is manufactured from piezoelectric polymer. Figure 1.5 shows the design of this type of harvester, in which the mechanical deformations caused by the motion of fluid forces stretching and compressing of the flag, which produces electricity. Secondly, a micro structured piezoelectric energy harvester is presented in the same study. Figure 1.6 represents the changing velocity of fluid flow produced pressure with changing amplitude on the PZT energy harvester. Pressure variation originates stress inside the piezoelectric layer, which in return produces electric charges on the electrodes. The basic idea proposed in the study is that different number of piezoelectric energy harvesters together with an AC-to-DC conversion mechanism setup are built up to modules in order to produce enough electrical energy which then can be used for many different applications. An example of piezoelectric energy harvesting is presented in [16], where an energy

scavenging scheme from moving fluid is illustrated in which cantilever oscillation converted kinetic energy into electrical energy.

Piezoelectric energy harvesters capture energy from the fluid flow, which makes them attractive for monitoring underwater pipelines with the help of sensors. Previous studies concentrated on extracting energy from harvesters, but they did not present scalable energy harvester design, which can produce a range of power for WSN. They also did not study performance impact on the pipe. This study addresses these aspects of research missing in the literature.

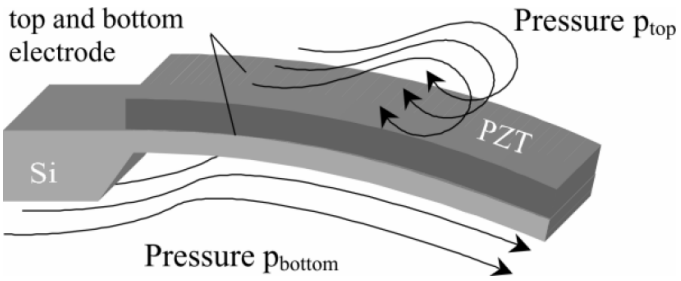

Figure 1.5. Piezoelectric bimorph generator [15].

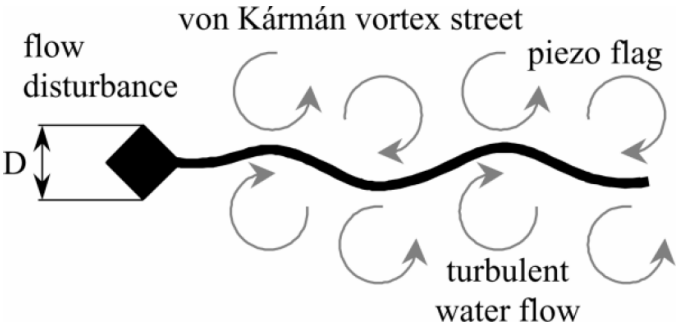

Figure 1.6. Moving flag subjected to flow disturbance in turbulent water flow.

1.5 Wireless Sensor Nodes

A sensor network is a group of nodes that are linked with each other using a communication infrastructure for either monitoring or control purposes. The communication infrastructure of a sensor network can be either wired or wireless. Batteries are primarily used to power these sensor nodes, but a main drawback of unconnected nodes is finite battery capability. In order to resolve this problem, nodes can use large batteries for longer lifetime. Nevertheless increased size, weight and cost of the battery are the major challenges. Numerous solution methods have been suggested to exploit the lifespan of sensor nodes, which use battery for their operation. Nonetheless, the lifetime remains restricted and limited [17]. A self-powered wireless sensor network is a sustainable and reliable option for in-pipe monitoring applications in case of underwater pipelines because energy harvester, which utilizes natural resources, is used in the system. Furthermore, sustainability aspect is enhanced because of “infinite” lifetime and continuity of supply in the network. Important system components for wireless sensor node are power source, transceiver, memory, transducer and microprocessor [4]. These sensors monitor different parameters of pipelines performance such as pressure, temperature and Ph. The configurations for a typical wireless sensor node and sensor network are shown in Figure 1.7. In order to operate wireless sensor node, the reliability and continuity of the power supply is very important. Additionally, the power source is a mandatory part of whole sensor node architecture in order to enable sensing, processing, storing, and transmission functions, which is shown in Figure 1.7. The three important subsystems of WSN node are computing, communication and sensing.

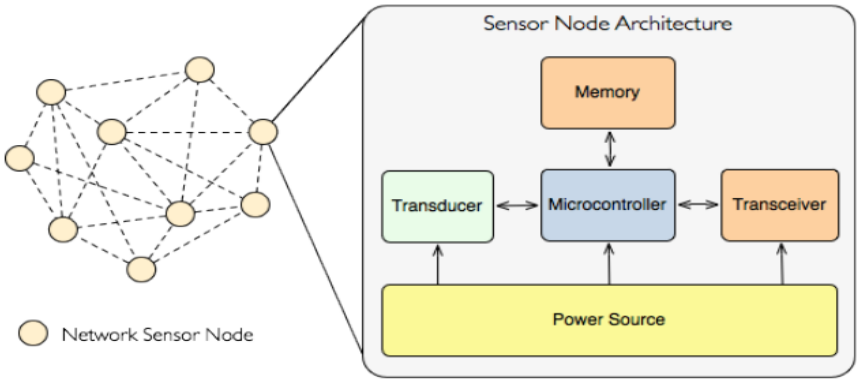

Figure 1.7. Typical architecture of sensor network and sensor node [18].

The major function of subcomponents of wireless sensor nodes is given below [4].

Transducer: It produces electrical signals in agreement with the measured value

Microcontroller: It processes data.

Memory: It store programs and important data.

Transceiver: It is responsible for receiving and transmitting data over the communication channel.

Power Source: It provides electrical power required for node operation.

Computing subsystem collects the measurement values using digital input and output signals or analog-to-digital converters, processes, and saves the data. It is used to coordinate the communication in the WSN as well. The microcontroller is the main component of the computing subsystem. Common microcontrollers and their voltage and power requirements are shown in Table 1.1. It can be seen from the table that computing subsystem has a range of 0.0054 mW to 230 mW power requirement.

Communication subsystem provides connection to other nodes and consists of a wireless transceiver and an antenna. This unit needs the most of the power consumption requirements as compared to other subsystems of the WSN. The two most popular medium used for communication subsystems are acoustic and radio transceivers [19] [21]. In case of acoustic transceivers, sensor nodes are connected to underwater basins with the help of wireless acoustic links and can operate without ropes, cables, or distant control, and thus they have a variety of real life usage in oceanography, environmental monitoring, and underwater resource study [22]. It is sometimes necessary to use acoustic transceivers such as in case of underwater systems because RF transceivers are attached through cables to surface buoys to come in the standard frequency range [18]. This creates security problems as the connection is wired through the cable and it may be damaged due to sea current and ships. Acoustic transceivers are integrated with the underwater pipelines infrastructure through WSN so there is no security issue while using these kinds of transceivers That is why, these systems are applicable for underwater pipeline applications. However, these kinds of transceivers have certain challenges such as they need higher power than RF transceivers due to greater distances and more difficult signal processing requirements. Power consumption requirements for both RF and acoustic transceivers are summarized in Table 1.1 and 1.2 respectively. It can be seen from the tables that RF transceivers require low power as compared to acoustic transceiver. Table 1.2 lists standard models of acoustic transceivers, and in addition compares the power needed by transceivers according to the distance of communication. All type of power consumption requirement including transmission (TX), receive (RX) and sleep power are summarized in this table for these transceivers.

Table 1.3 shows the three groups of RF transceivers that are categorized according to current consumption. The power requirement of sensing subsystem depends upon the type of sensors needed for monitoring purposes. The type of sensors and their power requirements that are important for underwater pipeline monitoring are summarized in Table 1.4.

Table 1.1 Power consumption requirements for some famous microcontrollers [19, 20].

CPU	**Voltage Supply (V)**	**Power Active (mW)**	**Power Down (µW)**	**Sensor Node**
4-Bit CPU				
EM6603	1.2-3.6	0.0054	0.3	
EM6605	1.8-5.5	0.012	0.9	
8-bit CPU				
Attiny 261 V/461 V/861 V	1.8-5.5	0.684	0.1	
PIC16F877	2-5.5	1.8	3	CIT
MC68HC05PV8A	3.3-5	4.4	485	
AT90LS8535	4-6	15	45	WeCRene
ATmega163L	2.7-5.5	15	3	Rene2Dot
ATmega103L	2.7-3.6	15.5	60	MicalBadge
C8051F311	2.7-3.6	21	0.3	Parasitic
ATmega128L	2.7-5.5	26.7	83.15	Mica2 Btnode
PIC8F452	2-5.5	40.2	24	EnOceanTCM
80C51RD+	2.7-5.5	28	150	RFRAIN
16-bit CPU				
MSP430F149	1.8-6	3	15	Eyes, BSN
MSP430F1611	1.8-3.6	4.36	2.86	Telos
MC68EZ326	3.3	60	60	SpotON
32-bit CPU				
AtmelAT91ARMThumb	2.7-3.6	114	480	
Intel PXA271	2.6-3.8	193	1800	iMote2
Intlel Strongarm SA100	3-3.6	230	25	WINµAMPS

Table 1.2 Power consumption requirements for Acoustic Transceiver [23-25].

	Center	Bandwidth	Bit Rate	Distance	TX	RX	Sleep	AT-WU		Size	
Model	**(kHz)**	**(kHz)**	**(bps)**	**(km)**	**(W)**	**(W)**	**(mW)**	**(mW)**	**Medium**	**Length (mm)**	**Diameter (mm)**
UWM100	35.695	17.85	17,800	0.35	1	0.75	8	8	Water	235.7	87.2
UWM2000	35.695	17.85	17,800	1.5	2	0.8	8	8	Water	249.7	
UWM2000H	35.695	17.85	17,800	1.5	2	0.8	8	8	Water	249.7	87.2
UWM2200	71.4	35.7	35,700	1	6	1	12	8	Water	160	126.2
UWM3000	10	5	5,000	3	12	0.8	8	8	Water	236	126
UWM3000H	10	5	5,000	3	12	0.8	8	8	Water	236	126
UWM4000	17	8.5	8,500	4	7	0.8	8	8	Water	286	144
UWM10000	10	5	5,000	10	40	0.8	9	8	Water	580	150
SC2R 48/78	63	30	31,200	1	18	1.1	2.5	5	Water	265	110
S2CR 40/80	51	26	27,700	1	40	1.1	2.5	5	Water	265	110
S2CR 18/34	26	16	13,900	3.5	35	1.3	2.5	5	Water	265	110
S2CR 12/24	18.5	11	9,200	6	15	1.1	2.5	5	Water	390	113
SC2R 7/17	12	10	6,900	8	40	1.1	2.5	5	Water	420	113
AQUA Modem 1000	9.75	4.5	2,000	5	20	0.6	1	5	Water	242	165
Micomodem (FSK)	25	4	80	2	100	0.23	0.2		Water	Unavailable in literature	
Micomodem (PSK)	25	5	5,388	2	100	2.23	0.2		Water	Unavailable in literature	
ATM 9XX (PSK)	11/18.5/24.5	5	2,400	6	20	0.768	16.8		Water	818	102
ATM9XX(MFSK)	11/18.5/24.6	5	15,360	6	20	0.768	16.8		Water	818	102
ATM885	18.5	5	15,360	0.7	84	0.7			Water	850	140
SAM-1	37.5	9	154	1000	32	0.168			Water	135	40
AquaComm Marlin	23	14	480	1	1.8	0.252	1.8	25.2	Water	80	70
AquaComm Mako	23	14	240	3	1.8	0.252	1.8	25.2	Water	80	70
AquaComm Orca	23	14	100	3	1.8	0.252	1.8	25.2	Water	80	70
Micronmodem	22	4	40	0.5	7.92	0.72			Water	56	79
Modem			1,000	0.1	1.2	0.024	0.003		Water	Unavailable in literature	

Table 1.3 Power consumption requirements for Radio Frequency Transceivers [19, 26].

Type	Clock [MHz]	Voltage(V)	Rx [mA]	Tx [mA]	Satndby Current [µA]
Low-power transcievers					
MPR300CB	916	3	1.8	12	1
SX1211	868-960	2.1-3.6	3	25	
TR1000	916	3	3.8	12	0.7
CC1000	315-915	2.1-3.6	9.6	16.5	1
Medium-power transcievers					
nRF401	433-434	3	12	26	8
CC2500	2400	1.8-3.6	12.8	21.6	
XE1205	433-915		14	33	0.2
CC1101	300-928	1.8-3.6	14.7	15	0.2
CC1010	315-915	2.9	16	34	0.2
CC2520	2400	1.8-3.8	18.5	17.4	<1
CC2420	2400	2.1-3.6	18.5	17.4/0	1
CC1020	402-915	2.3-3.6	19.9	19.9	0.2
CC2430	2400	2-3.6	19.9	19.9	
PH2401	2400	1.8	20	20	
nRF2401	2400	1.9	22		0.4
CC2400	2400	1.8	24	19	1.5
CC2530F32	2400	2-3.6	24	29	
RC1180	868	2-3.9V	24	37	
LMX3162	2450	3-5.5	27	50	
STD302N-R	869	3-5.5	28	46	
MC13191	2400	2.7	37		

Table 1.4 Power Consumption for sensors needed for sensing subsystems [26, 27].

Sensor Name	Type of sensor	Voltage range	Converstaion Current	Standby current	Power (Active)	Size (Length x Diameter)
MS5541C	Water Pressure Sensor Temperature	3V (2.2V-3.6V)	1mA	1µA	3 mW	6.2 mm x 6.4 mm
Signet 2350	sensor	5V (5V-6.5V)	1.5mA	5 µA	7.5mW	34 mm x 105 mm
Signet 2714-2717	pH/ORP sensor	4.5	1mA	1 µA	4.5mW	27 mm x 102mm

1.6 Objectives

Underwater pipelines are sources of transporting important resources such as water, oil and gas. If some kind of damage occurs to pipeline systems, there will be huge loss of important resources so it is very necessary to monitor these pipelines. Sensors are needed for monitoring purposes in order to ensure that everything is under control. There are various kinds of sensors such as pressure, temperature, and pH, which are used for underwater pipeline monitoring applications. This study proposes a near optimal scalable energy harvester capable of powering a wireless sensor node for in-pipe monitoring applications of Turkey-Cyprus water pipeline project. The most important aspect of this study is that an efficient energy harvester near optimal design is presented, which would be then coupled with rest of the system components with commercially available specifications to make a reliable self-powered node for in-pipe monitoring applications. Reference [12] discussed the vertical axis wind turbine for getting power from water flowing inside the pipes, but the pipe specifications and water flow rate considered in that case was completely different from Turkey- Cyprus pipeline project. So, this study would be different from that study as piezoelectric energy harvester scalable and near optimal design is presented in this study. In addition, performances impact on the pipe for installing an energy harvester is also studied in detail in terms of head loss which is one of literature gaps as mostly literature investigates power output of the energy harvester. The schematic diagram of Turkey-Cyprus pipeline project is shown in Figure 1.8. The pipeline is 80 km long, which consists of pipes made of Polyethylene and single pipe is 500 m long with an outside diameter of 1600 mm [29].

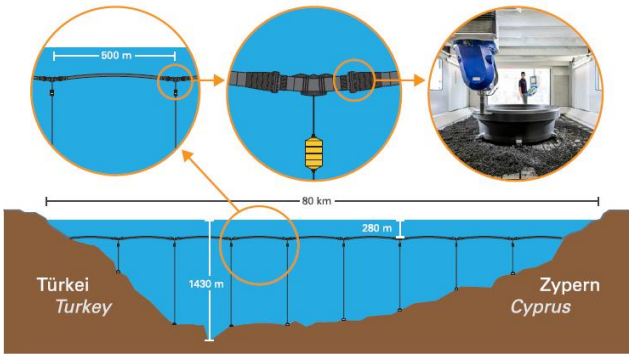

Figure 1.8. Schematic diagram Turkey-Cyprus underwater pipeline project [28].

1.7 Overview of the Thesis

The thesis is organized as follows. In Chapter 2, both piezoelectric and electromagnetic energy harvesters are compared and analytical calculations are performed to predict the performance of the energy harvesters. In addition, why piezoelectric energy harvesters are preferred in this study is also discussed. Chapter 3 presents the detailed analysis of PZT energy harvester in COMSOL software. Detailed analysis includes complete geometric modeling of energy harvester, meshing and post processing of results. The velocity distribution, pressure distribution and tip displacement results are discussed in Chapter 3, which determines the resultant power required to operate wireless sensor nodes. Chapter 4 illustrated the performance impact of energy harvester on the pipe and analyses how much velocity and pressure is disturbed by the presence of energy harvester. In addition, the performance impact is also investigated in quantitative terms of head loss in the same chapter. Chapter 5 concludes the thesis.

Chapter 2 - ANALYTICAL MODELS

Analytical calculations are performed for both electromagnetic and piezoelectric energy harvester to find the dimensions and power needed to operate the wireless sensor nodes. All the analytical calculations are done by using the equations present in the literature to find the maximum power achievable from both types of energy harvesters.

2.1 Analytical Model for Electromagnetic Energy Harvester

2.1.1 Literature Review of Micro Turbines

Different commercial turbines with small dimensions are studied in this section. Vertical axis water turbine installed in pipeline is shown in Figure 2.1, where it is embedded into the pipe together with other mechanical and electrical parts [12]. This type of turbine affect the fluid flow significantly since it is completely embedded into the pipe. There are many types of water turbines which have different standard specification of head and flow rate and the most commonly used among them are Francis, Kaplan and Pelton turbines. Figure 2.2 show that Kaplan turbine is the most attractive option for the water duct because it produces electrical power at small flow rate and water head. But the major drawback of Kaplan turbine is that it impacts the environment by altering the trail of fluid flow. One of the turbines produced by *Seamap* Company is UW-100 Pico hydro turbine and is used to generate power for the wireless sensors [29]. It can be seen from Figure 2.3 that this kind of water turbine has a very important advantage that it will not alter the path of fluid flow. But some of its electrical

components are immersed in the drinking water which creates water pollution and people cannot drink that water.

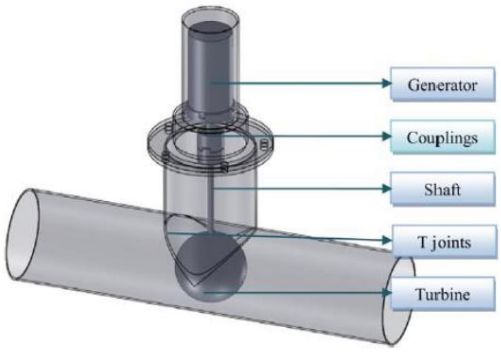

Figure 2.1. System having turbine embedded into the pipe [12].

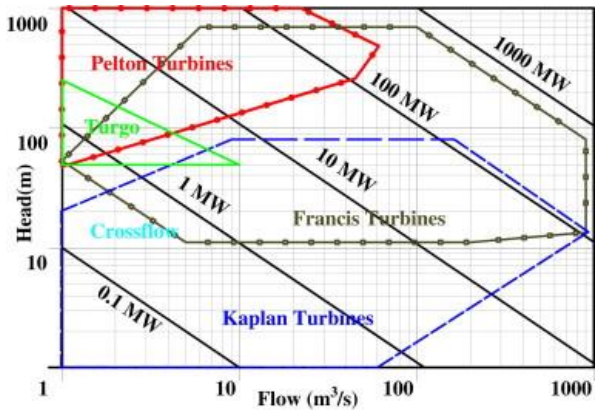

Figure 2.2. Turbine application chart [8].

Figure 2.3. UW 100 turbine [29].

A revolving and a changing flux energy harvester using a three-phase generation for transforming energy from water in residential water pipes are presented in another study [30]. The energy harvester is used to operate a smart metering system connected to the underground to make the whole system self-governing from exterior power supplies or limited lifetime batteries .The energy harvester designed in this study has the capability to produce power ranging from 15 mW at 5 liter per minute to 720 mW at 20 liter per minute.

Some of the commercially produced micro turbines are presented in Table 2.1. This table consists of turbines having smaller dimensions and capability to produce enough power to operate wireless sensor nodes for underwater pipeline monitoring applications.

Table 2.1 Commercial turbines for pipeline monitoring applications [12, 29, 30, 31].

Turbine Type	Turbine Diamter (mm)	Startup Velocity (m/s)	Max. Power Production (W)
UW-100	312	1.5	100
Drag type 5 blade turbine	92	1.5	12
Drag type 6 blade turbine	92	1.5	32.2
Drag type 12 blade turbine	92	1.5	88.2
Rotational radio flux energy harvester	20	1.061	0.72
MT100	350	0.031181	100
MT350	350	0.044693	340
MT650	480	0.033953	650
See Studion	90	0.052397	1.08

2.1.2 Analytical Model

The power produced by the machine using electromagnetic energy is given in Equation 2.1 where the kinetic energy is *E*, time is *t*, and the efficiency of the machine is η.

$$P = \eta \times \frac{E}{t} \tag{2.1}$$

Moreover the equation of kinetic energy, mass and volume are expressed in Equation 2.2, 2.3 and 2.4 [9] to visualize the main equation which is used for finding power. Kinetic energy is given by

$$E = \frac{1}{2} m v_f^2 \tag{2.2}$$

where m = mass of the fluid; v_f = fluid velocity flowing in duct. Mass of fluid is simply multiplication of density ρ and volume V.

$$m = \rho V \tag{2.3}$$

Volume of fluid is related to the turbine area $A_{turbine}$ and fluid velocity

$$V = A_{turbine} v_f \tag{2.4}$$

Substituting Equation 2.2, 2.3, and 2.4 in to Equation 2.1 gives the Equation 2.5. This equation is used to find to power needed to operate the WSN.

$$P = \frac{1}{2} \eta \rho A_{turbine} v_f^3 \tag{2.5}$$

2.1.3 Typical Area Needed for Micro Turbine

The efficiency of the hydro turbines varies from 75 to 95 percent depending upon the size of hydro turbine [11]. Turkey-Cyprus water pipeline flow conditions are taken in to account where velocity of water is taken as 1.4 m/s, density of water is 1000 kg/m^3. Both upper and lower case efficiencies are taken in to consideration to calculate the area needed for the turbine presented in Table 2.2 to analyze the area needed for the range of different power requirements needed for WSN. Power range is taken from 1 W to 20 W to estimate the area needed for the turbine according to equation 2.5. The area varies from 9.74 cm^2 to 194 cm^2 depending upon power requirements of WSN. But this area is subject to change according to specification and efficiency of hydro turbine.

Table 2.2 Turbine area needed to find power range from 1W to 20 W.

P (W)	Area (cm^2) for η=75%	Area (cm^2) for η=95%
1	9.718172983	7.672241829
2	19.43634597	15.34448366
3	29.15451895	23.01672549
4	38.87269193	30.68896732
5	48.59086492	38.36120915
6	58.3090379	46.03345097
7	68.02721088	53.7056928
8	77.74538387	61.37793463
9	87.46355685	69.05017646
10	97.18172983	76.72241829
11	106.8999028	84.39466012
12	116.6180758	92.06690195
13	126.3362488	99.73914378
14	136.0544218	107.4113856
15	145.7725948	115.0836274
16	155.4907677	122.7558693
17	165.2089407	130.4281111
18	174.9271137	138.1003529
19	184.6452867	145.7725948
20	194.3634597	153.4448366

2.2 Analytical Model for Piezoelectric Energy Harvester

2.2.1 Assumption Used for Dimension of Bluff Body

The bluff body generates flow disorder by interrupting the fluid flow and produces tumults. In addition, it supports the cantilever naturally. Bluff body produces turbulences in the fluid due to which the rotating whirls called “von Karman’s” vortex street are created at Reynolds Numbers (Re) between 50 and 10,000 [32]. Beyond these Higher Re numbers the release of the twirls develops extra irregular and random that converts the fluid movement into a turbulent flow regime. At lower Re numbers viscous forces dominate and twirls cannot develop. The dimension *D* of the bluff body depends on the density ρ, the dynamic viscosity η, Reynolds Number *Re* and the velocity *v* of the fluid. Equation 2.6 shows the dimension of bluff body relation [33].

$$D = \frac{(\mathrm{Re})(\eta)}{(v)(\rho)} \tag{2.6}$$

2.2.2 Assumptions Used for Calculating Length of Cantilever Beam

The frequency of the vortex shedding depends upon the dimension of bluff body *D*, the flow velocity *v* and the Strouhal number *Sr*. and its formula is shown in Equation 2.7 [34].

$$f = \frac{(Sr)(v)}{D} \tag{2.7}$$

Velocity reduction takes place due to presence of energy harvester and it is assumed that average velocity is decreased by 15% and the twirls after the flow disorder traveling only with 85% of the flow velocity due to presence of bluff body [35]. This needs to be considered because it decreases the flow velocity. The period of the "von Karman's" vortex street λ, which is represented in Equation 2.8, is found by taking this factor into account.

$$\lambda = \frac{0.85v}{Sr\frac{v}{D}} = 4.25D \tag{2.8}$$

If cantilever length is very long then it will not oscillate in the first harmonic mode and the higher oscillation modes could lead to accumulation of charges in only one layer and thus no electric voltage at the corresponding electrodes. Hence, it is compulsory to reduce the length of the cantilever L to half of the vortex-tear-off wavelength. Under these conditions we can find a relation for the optimal L to D ratio which is given in Equation 2.9 [32].

$$\frac{L}{D} = 2.125 \tag{2.9}$$

2.2.3 Assumption Used for Calculating Pressure

The pressure difference Δp is represented in Equation 2.10 assuming that the velocity component of the fluid which is rotational of the twirls is about one third of the flow velocity of the uninterrupted fluid [36].

$$\Delta p = \frac{\rho}{2}((v - \frac{v}{3})^2 - v^2)) \tag{2.10}$$

2.2.4 Assumption Used for Minimum Thickness

Minimum thickness T_{PZTmin} of the energy harvester is obtained from the extreme bend and the ultimate tensile strength of the PZT-material σ_{max} which is shown in Equation 2.11 [33].

$$T_{PZT\min} = \frac{1}{2}\sqrt{3\Delta p \frac{L^2}{\sigma_{\max}}} \tag{2.11}$$

2.2.5 Assumption for Tip Displacement

Tip displacement of a cantilever beam is expressed in terms of length, Young's Modulus *Y*, pressure difference Δp, and thickness of the beam T_{PZT} as follows [33].

$$T = \frac{\Delta p}{16.Y.{T_{pzt}}^3}(L^4 - 4L^4 + 6L^3) \tag{2.12}$$

2.2.6 Mechanical Energy and Electrical Energy Equations

Energy transformation takes place during the bending of the cantilever only. During this period a portion of the mechanical energy W_m is converted to electrical energy W_{el}. The mechanical energy and electrical energy relations are presented in equation 2.13 and 2.14 [15].

$$W_m = \frac{3}{80}\Delta p^2 \frac{BL^5}{T_{pzt}^3 Y} \ , \tag{2.13}$$

$$W_{el} = \frac{1}{128}\Delta p^2 \frac{d_{31}}{\varepsilon_0 \varepsilon_r}\frac{BL^5}{T_{pzt}^3} \ , \tag{2.14}$$

where Y, T_{pzt}, B, L, and ρ are Young's modulus, thickness, width, length and density of beam, respectively. The energy harvesting efficiency is found from the Equation 2.15. Electrical energy to mechanical energy conversion ratio relies on only properties of material. It shows the significance of the piezoelectric constant d_{31} and provides an indication about the transformation productivity of the piezoelectric scavengers [32].

$$\frac{W_{el}}{W_{mech}} = \frac{5}{24}\frac{Yd_{31}^2}{\varepsilon_0\varepsilon_r} \tag{2.15}$$

where ε_r: relative dielectric constant, ε_o: Absolute Permittivity, d_{31}: piezoelectric strain Constant.

2.2.7 Power and Frequency Calculation

The frequency of vibrations affect the electrical power. Uneven pressure fluctuations force the beam to bend in both clockwise and anticlockwise direction continuously with the frequency given in Equation 2.16 [37].

$$f_{beam} = \frac{1}{2\pi}\sqrt{\frac{35}{33}\left(\frac{YT_{pzt}^2}{L^4\rho}\right)} \tag{2.16}$$

The electrical power output P_{el} depends upon frequency and electrical energy output from the energy harvester [33] and is shown in Equation 2.17.

$$P_{el} = 8 f_{beam} W_{el} \tag{2.17}$$

2.3 Reason for Choosing Piezoelectric Energy Harvester for Further Analysis

Electromagnetic energy harvester needs to rotate for production of energy and it requires regular maintenance. This type of energy harvester cannot be used for the applications which are difficult to access such as underwater or underground pipelines. Piezoelectric energy harvesters are rotation-free structures having the ability to continuously vibrate and produce electrical energy on regular basis with minimal maintenance requirements so that is the main reason for choosing them for further analysis in this research.

2.4 Power Electronics Circuits for Piezoelectric Energy Harvester

Jinhao et al. [38] compared four different types of power electronics circuits for the vibration based PZT energy harvesters. According to this study, synchronized switching technique brings major enhancement in terms of efficiency to vibration-based PZT harvesting systems. Different configurations of PZT energy harvester based power electronics circuits proposed in this study are depicted in Figure 2.4. It can be seen from Figure 2.4 (a) that the classic interface circuit comprises a diode rectifier and filter capacitor. The tip displacement should be purely sinusoidal in order to get completely rectified output from this type of circuit. The Cockroft-Walton voltage doubler circuit is presented in Figure 2.4 (b). It produces high voltages from a low voltage AC source, which is useful for applications where electric loads with large resistance needs to produce large power. Synchronous charge interface circuit is shown in Figure 2.4 (c).

The principle of synchronous charge extraction (SCE) is to transfer electric energy gathered on the capacitor C_0 of the piezoelectric element to energy storage element intermittently. A main advantage of using this method is that the sporadic extraction of energy is matched with the mechanical vibration. The potential challenge of controlling circuit is to turn on and turn off the switch properly at the right time. Solution of this type of circuit is presented in Figure 2.4 (d) where PNP and NPN transistors are used for triggering circuit.

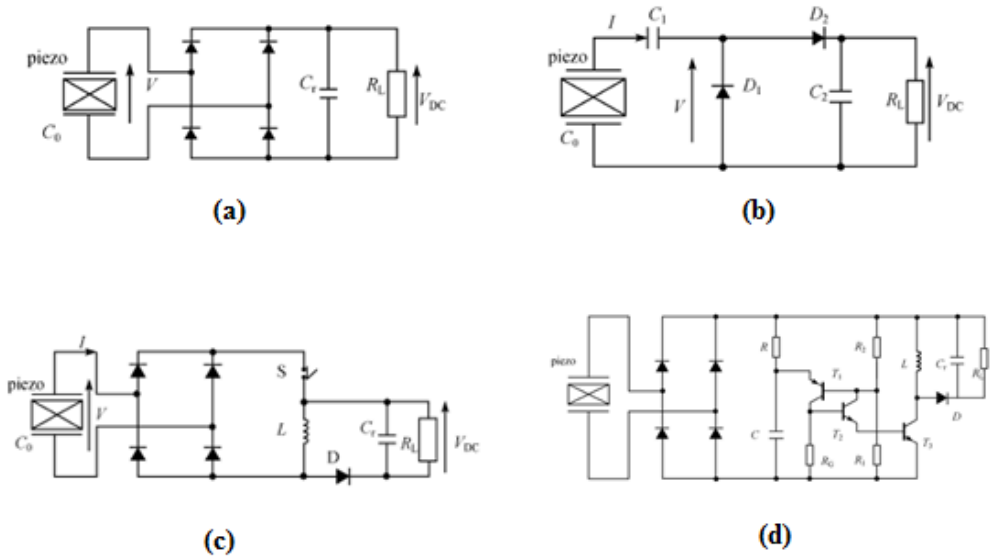

Figure 2.4 (a) Classic interface (b) Voltage doubler interface (c) Synchronous charge extraction interface circuit (d) Switch trigger circuit for synchronous charge extraction.

Different power electronics conversion circuits are investigated in the literature which are compared in Table 2.2 with respect to their features and performance evaluation [38, 39, 40]. This table shows that energy harvester voltage doubler, and buck boost sensor less energy harvester circuits have high efficiency, with requirement of single supply voltage. Both of these power conversion circuits are compatible with micro-scale

integration. However, buck boost energy harvester circuit has highest efficiency of 84% among all circuits but it is not able to adjust with rectified voltage. On the other hand, voltage doubler energy harvester circuit has lower efficiency of 60%, but able to synchronize with rectified voltage. Hence, power conversion mechanism is selected based on many factors, including input waveform frequency, power and voltage constraints, as well as power and voltage output requirements.

Table 2.3 Comparison of different types of PZT harvester power electronics circuits.

Power Conversion Method	**Features**
Standard Full bridge rectifier	Very low efficiency and circuit is not able to adjust rectified voltage to extract maximum power so non adaptive. No external supply is required and compatible with microscale integration, Standalone operation
Voltage Doubler	Low efficiency with non adaptive problem. Implemented as Complementary metal–oxide–semiconductor (CMOS) chip
Optimized energy harvester for a full bridge recrifier using step down converter	Multisupply voltage required for operation with efficiency fairly high with as compared to first 2 methods
Adaptive energy harvester for a full bridge recrifier using step down converter	Need multisupply voltage but the circuit is adaptive. Efficiency and losses have not been discussedin this study
Buck Boost Sensorless Energy harvester	Sensorless and non adaptive. Efficiency above 84% for given piezolectric parameters. Also compatible with microscale integration
Synchronized switch harvesting	Efficiency of 70% with 5% power consumption. But the circuit is non adaptive and needs multi supply voltage
Adaptive energy harvester using voltage doubler	Efficiency of 60% and the circuit is adaptive with single supply voltage. The circuit is also compatible with microscale integration

Chapter 3 - FINITE ELEMENT MODEL AND ANALYSIS

A sensitivity analysis is done to design a near-optimal piezoelectric energy harvester to power underwater in-pipe WSN, and the results are verified through finite element simulations and analytical equations in this chapter. The derived energy harvester topology is scalable to the requirements of power generation, and naturally has increased impact to the performance of the pipeline carrier as its dimensions are increased. The near-optimal design in this study generates power between 0.02 mW to 0.82 mW when velocity of 1.4 m/s is applied at the inlet under turbulent flow conditions. Reynolds number should be less than 10,000 to observe the von Karman's street [32]. Two types of bluff bodies I-shaped and D-shaped are compared with respect to power requirements to determine which type is most suitable for pipelines.

The bluff body causes flow disorder and supports the cantilever beam naturally so it is an essential part of the PZT energy harvester. It interrupts the normal fluid flow and generates flow disturbing bodies "von Karman's" vortex street. Firm "von Karman's" vortex streets are observed at Reynolds-Numbers (Re) between 50 and 10,000 [33]. PZT energy cantilever beams should produce continuous vibrations for generation of electrical power. Figure 3.1 presents the diagram of working principle of PZT Energy harvester. It depicts that the flow passes over the bluff body and a pattern of sporadic vortices is generated at each side of the bluff body. As a result, cantilever beam starts to vibrate in both clockwise and anticlockwise direction in a periodic manner.

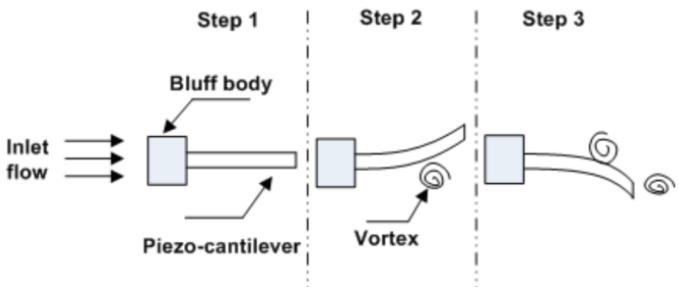

Figure 3.1 Schematic diagram of PZT energy harvesting [36].

3.1 Model Description

Two types of bluff bodies D-shaped and I-shaped are used for the comparative analysis of power output produced since they can support the PZT cantilever easily. This study is only limited to these two types of bluff bodies but other types such as circular, triangular can also be used but their performance should be optimized using computational models. Figure 3.2 illustrates a PZT energy harvester supported by D-shaped bluff body operating in a fluid flow. Bimorph PZT energy harvester vibration energy is converted to electrical energy due to von Karman's street generation. Based on the specifications of the selected Turkey-Cyprus water pipeline as the case study, velocity of 1.4 m/s is applied at the inlet and pressure of zero is provided at the outlet.

Fluid-structure interaction (FSI) with turbulent flow is solved using a finite element software. The fluid enters the fluid domain through the inlet, interacts with bluff body to generate continuous vibrations to produce electrical power, and then

leaves at the outlet. Table 3.1 presents the necessary specifications of Turkey-Cyprus water pipeline which is used for further analysis in this study [28].

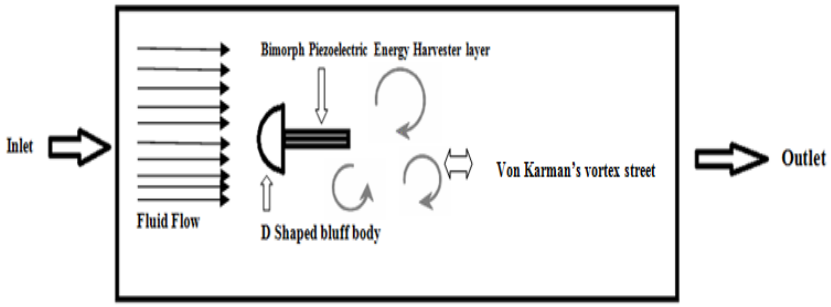

Figure 3.2. Schematic diagram of PZT energy harvester operation in fluid flow.

Table 3.1 Specification and material used for Turkey-Cyprus water pipeline project.

Pipe Parameters	**Numerical Value**	**Units**
Diameter	1.6	m
Velocity	1.4	m/s
Flow	2.38	m^3/s
Length of pipeline	80	km
Pipe wall thickness	6.4	cm
Material parameters		
Fluid	Water	
Pipeline	High-density polyethylene	
Energy Harvester Cantiliver	Polyvinylidene fluoride	
Bluff Body	Silicon	

3.2 Finite Element Simulation Results

A finite element simulation is carried out using PZT energy harvester in this section. As per design presented in the second chapter, the maximum dimension of the bluff body (*D*) is 7.142 mm and length of cantilever (L) is 15mm. The thickness of the energy harvester (*T*) is 0.35 mm according to ratio taken in [32, 33]. Table 3.2 presents the geometric properties of energy harvester and fluid channel made in COMSOL software.

Table 3.2 Geometric properties of fluid and energy harvester.

Modeled Parts	Property	Numerical Value (mm)
Fluid Channel Section	Length	200
	Height	80
Cantilever Beam	Length	15
	Thickness	0.35
Piezoceramic Layer on Beam	Length	15
	Thickness	0.35
D-shaped Bluff Body	Diameter	7.14

Cantilever beam used in the energy harvester is made of plastic based PZT material named polyvinyl di fluoride (PVDF) because it vibrates with a little force and handles high mechanical strain level without any damage [16]. It is not feasible to use ceramic based PZT material for the cantilever beam as they are rigid, brittle and heavy, causing restrictions in this kind of applications where flexibility is compulsory [41]. Bluff body is made of solid silicon material to support the cantilever. Turkey-Cyprus pipeline is transporting water so its material properties are used in the model for fluid domain. Material properties of the model are presented in Table 3.3.

Table 3.3 Material properties of fluid channel and energy harvester.

Domain	Property	Numerical Value	Unit
Fluid	Density	100	kg/m^3
	Dynamic Viscosity	0.001	Pa. s
D Shaped Bluff Body	Young Modulus	150	GPa
	Poisson's Ratio	0.33	
	Density	2330	kg/m^3
PVDF	Young Modulus	2	GPa
	Poisson Ratio	0.34	
	Density	1780	kg/m^3

Meshing is an important part of the design and automatic meshing is done for this analysis since expected results came after applying this mesh [42]. A sensitivity analysis with respect to the number of elements is performed for the mesh to ensure that the results obtained from finite elements model are correct. Figure 3.3 shows a graph plotted between pressure difference across the surface of cantilever and number of elements of mesh produced in automatic physics controlled fluid dynamics mesh produced in COMSOL. It can be seen from the graph that pressure difference results asymptotically approach to a constant value after 4000 finite elements. Figure 3.4 shows the model where uniformly distributed mesh is applied. The distribution of the mesh near to the D-shaped bluff body is much finer as compared to other regions of the fluid domain which is the main point of interest in this analysis.

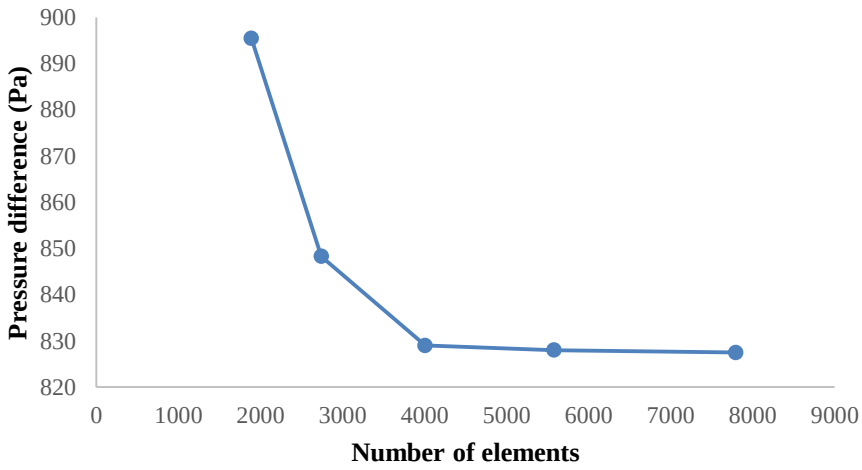

Figure 3.3. Sensitivity analysis of mesh with respect pressure difference across the surface of cantilever versus number of elements of mesh.

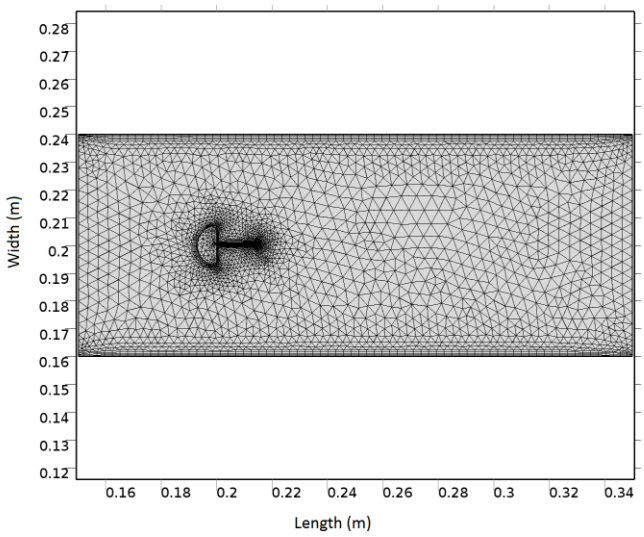

Figure 3.4. Mesh for D-shaped bluff body energy harvester model.

Figure 3.5 shows the generation of von Karman Street due to presence of energy harvester in the fluid flow. Velocity variation from 2.2 m/s to 0.2 m/s is produced near to the energy harvester due to presence of bluff body. After approximate distance of 0.1 m from the energy harvester average velocity of 1.39 m/s is observed at the outlet.

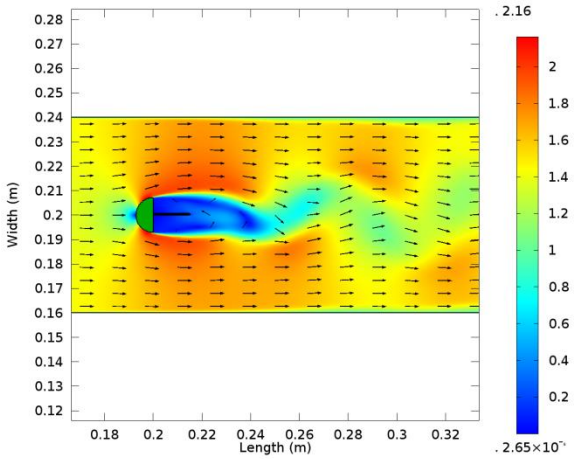

Figure 3.5. Finite element simulation results for D-shaped bluff body energy harvester velocity distribution (m/s) in the fluid domain.

According to analytical predictions the frequency of the PVDF energy harvester is 27 Hz and the pressure difference is 544 Pa. The power output is 0.46 mW for the designed model. Figure 3.6 shows the 5 points to get the data of the pressure across the surface of cantilever. The spatial average of pressure is found from these points to approximate the pressure at the surface of cantilever. The average pressure across the surface is 830 Pa resulting in the output power of 0.82 mW for the simulated model. Figure 3.7 represents the line graph extracted from the 5 data points. It shows continuous pressure variation which is necessary to extract energy from the PZT harvester. Frequency of oscillation of cantilever is 20 Hz which is found from tip displacement results as shown in Figure 3.8.

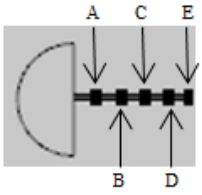

Figure 3.6. Five equidistant points monitored at both surfaces of the D-shaped bluff body energy harvester.

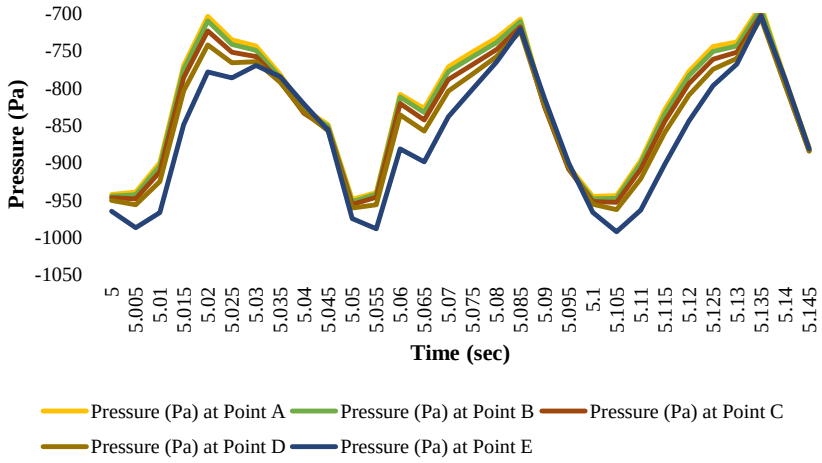

Figure 3.7. Extracted data points of pressure across the surface of D-shaped bluff body energy harvester layer from finite element simulation.

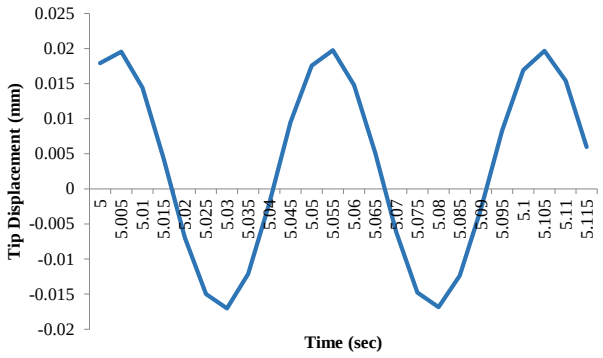

Figure 3.8. Tip displacement (mm) versus time (sec).

A finite element comparison between I-shaped and D-shaped bluff body is done in terms of power generation and impact to the fluid flow in underwater pipelines such as the one between Turkey and Cyprus. The rectangular conduit fluid domain is 0.2 m long and 0.05 m wide for the finite element model. Physics controlled mesh having 5592 domain elements and 297 boundary elements is applied with uniform distribution of elements as shown in Figure 3.9.

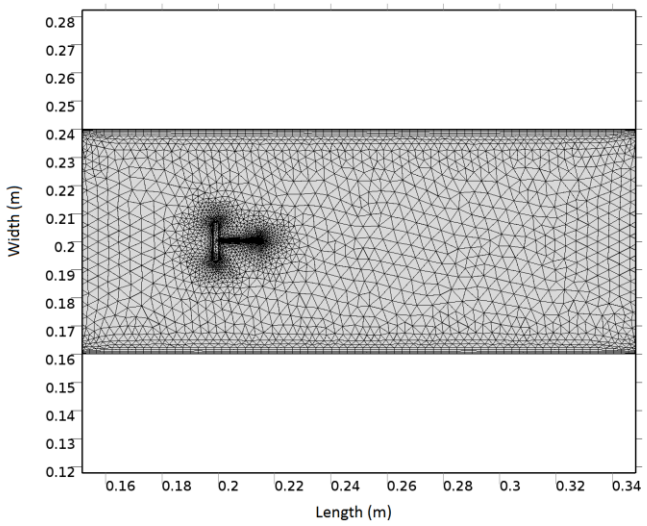

Figure 3.9. Mesh for I-shaped bluff body energy harvester model.

Figure 3.10 shows finite element results of PZT energy harvester having I-shaped bluff body. It illustrates the von Karman's street generation with significant variations in velocity from 0.1 m/s to 2.5 m/s near to boundaries of fluid domain. Large disturbance in velocity lasts until the fluid leaves at the outlet. Figure 3.11 shows 5 points inserted in to the cantilever beam through which spatial average pressure was found.

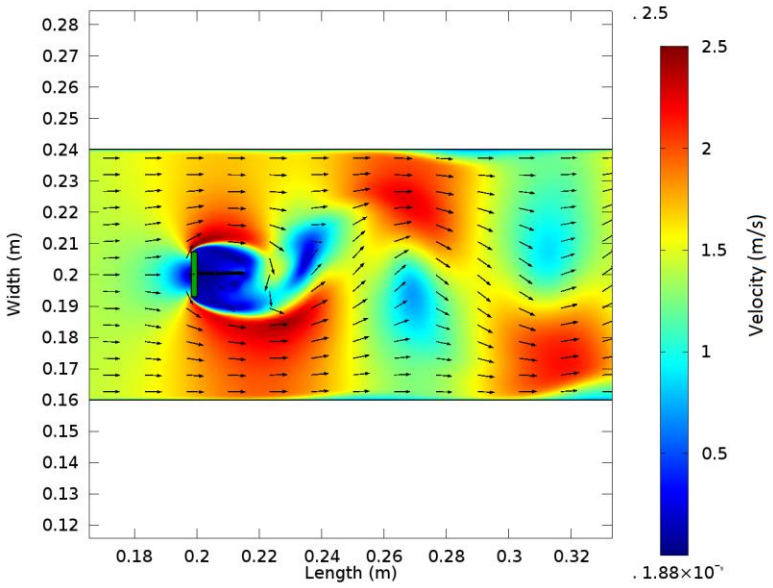

Figure 3.10. Finite element simulation results for I-shaped bluff body of velocity distribution (m/s) in the fluid domain.

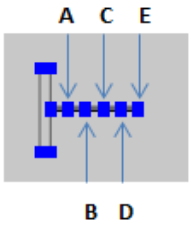

Figure 3.11. Five equidistant points monitored at both surfaces of the I-shaped bluff body energy harvester.

Figure 3.12 represents the line graph, which shows continuous oscillations with average pressure of 1630.45 Pa. Simulation results indicate that PZT energy harvester with I-shaped bluff body generates 2.24 mW, while D-shaped bluff body produces only 0.82 mW of power.

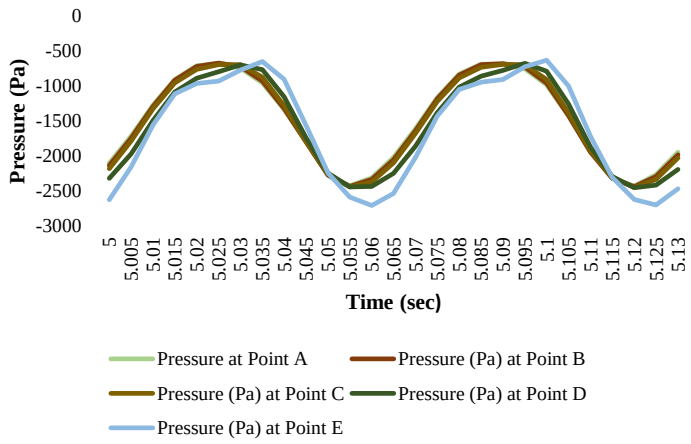

Figure 3.12. Extracted data points of pressure across the surface of I-shaped bluff body energy harvester layer from finite element simulation.

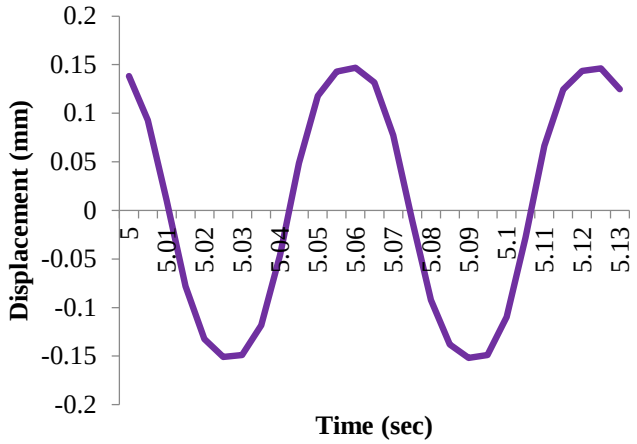

Figure 3.13. Tip displacements (mm) versus time (sec).

3.3 Sensitivity Analysis for Larger Power Production and Verification of Analytical Calculations

A sensitivity analysis is performed for the length of cantilever beam to extract maximum power from the energy harvester. The dimension of bluff body is taken

according to length to dimension ratio to ensure maximum power generation. Reynolds number is kept less than 10,000 for the necessary von Karman's street generation. The length of the cantilever beam is both increased and decreased by 50% in order to see the power generation results for energy harvester.

3.3.1 Finite element results for length increased by 50%

The length of the cantilever beam according to analytical calculations is 15 mm. It is increased to 50% in this step so the length is extended to 22.5 mm. No von Karman's street generation is observed which shows that Length to Dimension ratio of 2.125 is necessary to produce vibrations in the cantilever. The power produced by energy harvester having 15 mm length is 0.82 mW. Figure 3.14 shows the random behavior of the tip displacement results instead of continuous periodic oscillations for the increased length. It is due to oscillation of the cantilever in the higher harmonics mode than first harmonics where node and antinode of the tip displacement oscillations are cancelling each other and cantilever is bending at one end. Frequency which is necessary for the power generation cannot be calculated. This power cannot be further increased by increasing the length of cantilever since von Karman's street is not generated in this analysis. Figure 3.15 shows finite element results for this analysis. That is why; if the length of cantilever is increased to 50%, no power is generated.

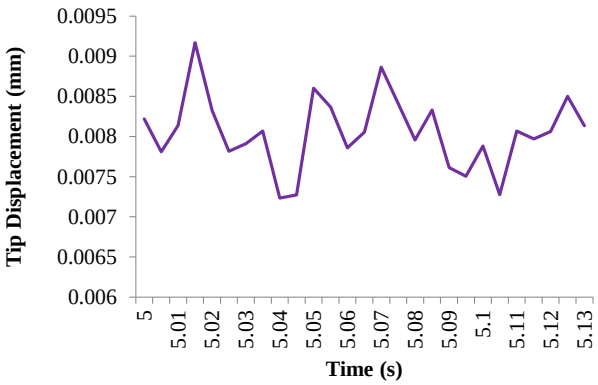

Figure 3.14. Tip displacement (mm) versus time (sec).

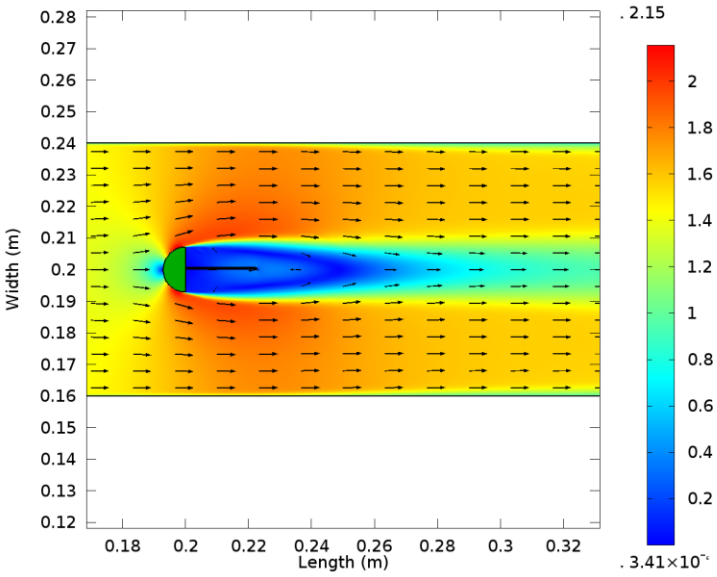

Figure 3.15. Finite element simulations for velocity distribution in the presence of energy harvester with a length of 22.5 mm.

3.3.2 Finite Element Results for length decreased by 50%

Length of the cantilever beam is decreased to 7.5 mm in this step. Figure 3.16 shows von Karman's street is generated which is compulsory for continuous electrical

power production. The average pressure across the surface is 1300 Pa as shown in Figure 3.17. This pressure is found from the 5 equidistant points inserted on the surface of cantilever in the finite element model. The frequency is found from the tip displacement results of the finite element simulation which is 23 Hz as presented in Figure 3.18. The power is decreased to 0.028 mW due to shorter length, which shows that power is strongly dependent upon the length of cantilever. This analysis confirms that length to dimension ratio of 2.125 is necessary to extract maximum power from the energy harvester.

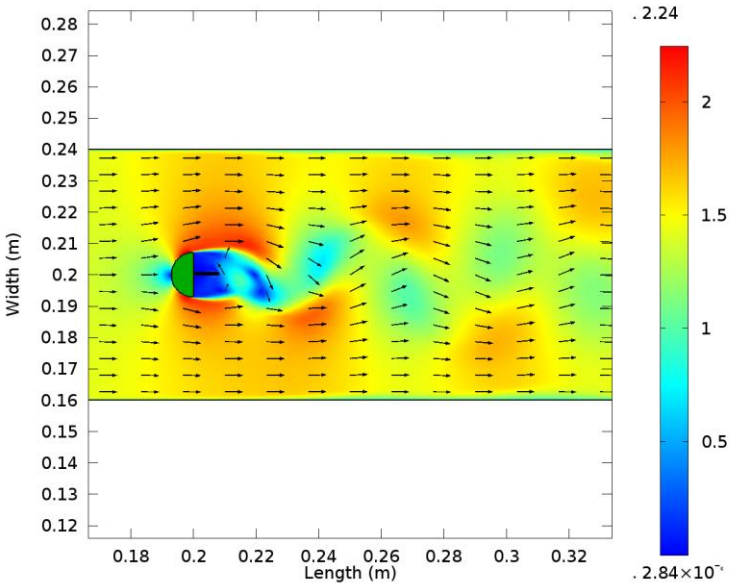

Figure 3.16. Finite element simulation for velocity distribution in the presence of energy harvester with a length of 8 mm.

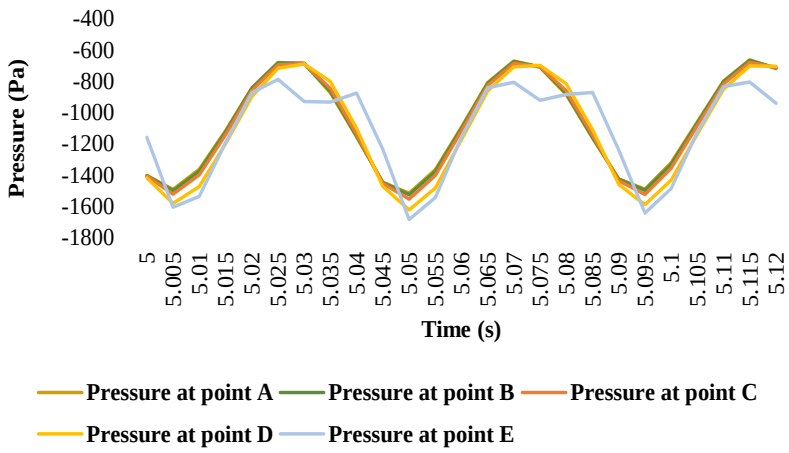

Figure 3.17. Extracted data points of pressure across the surface of D-shaped bluff body energy harvester layer from finite element simulation for length of 0.0075 m.

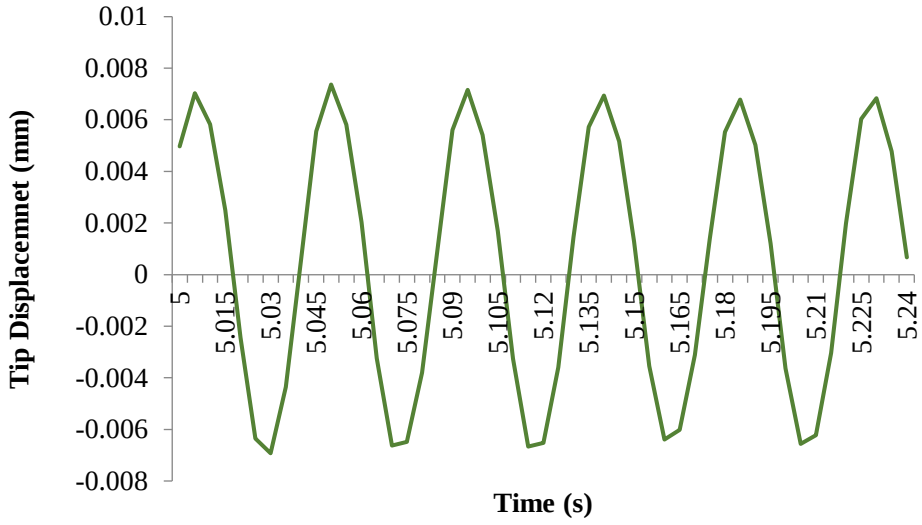

Figure 3.18. Tip displacement (mm) versus Time (sec).

3.3.3 Comparative analysis for Power Output results of different lengths

The simulation results are compared with the analytical calculations for each cantilever size. It can be observed from Table 3.4 that maximum power output is obtained from the dimensions designed from analytical calculations, although the actual value of the generated power differed due to simplifying assumptions in the analytical model. For a length of 5 mm finite element software gives error due to very short length and for 22.5 mm length pressure oscillations are damped which means that cantilever beam will not be able to vibrate continuously. A simulation with a length of 17.5 mm is also performed but tip displacement results are not periodic thus frequency cannot be calculated. So, 15 mm length is considered to be near optimal length, which is also consistent with the analytical predictions.

Table 3.4 Comparison of power output of analytical calculations and finite element analysis results for different lengths of the energy harvester.

Length of Energy Harvester (mm)	Simulation Power Found (mW)	Analytical Power Calculated (mW)
15	0.82	0.46
14	0.56	0.36
13	0.42	0.29
12	0.33	0.23
8	0.065	0.06
6	0.02	0.028

The finite element simulation results of power differed from the analytical predictions because pressure difference across the surface of the cantilever is not the same as the estimated pressure. It is because the dimension of bluff body is missed in

the Bernoulli equation while in finite element simulations pressure is disturbed due to presence of bluff body. Similarly, finite element simulation results of frequency are different from the frequency calculated from analytical equation, because *L* to *D* ratio of 2.125 changes when the length of cantilever is changed.

3.4 All possible 2D arrangements of energy harvester simulation analysis

An array of 5 energy harvesters in series with equal distance of 0.1 m is arranged in fluid domain to do first analysis. The dimension of rectangular conduit is: 0.6 m x 0.4 m. Figure 3.19 shows physics controlled fluid dynamics mesh of the finite element model, which consists of 30046 domain and 971 boundary elements.

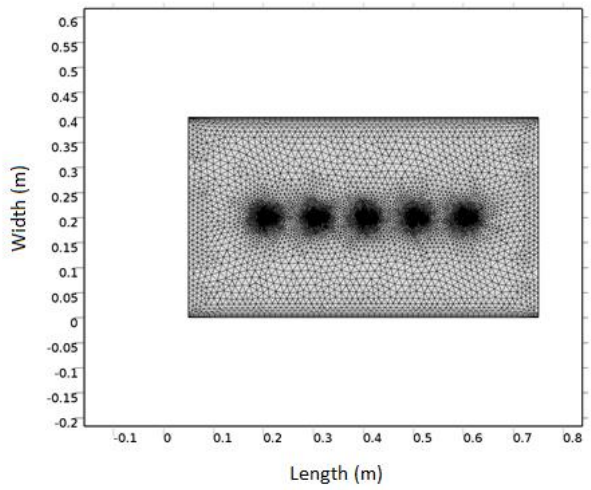

Figure 3.19. Mesh for multiple cantilevers in series energy harvester model.

Figure 3.20 illustrates the results of finite element simulation where 2 energy harvesters out of 5 are capable of producing continuous energy. It concludes that this type of combination of energy harvesters is not feasible for the Turkey-Cyprus pipeline project since at the 3rd energy harvester no von Karman's street pattern is observed.

This combination of energy harvester is able to produce only 1.50 mW at the expense of head loss of 88.2 mm.

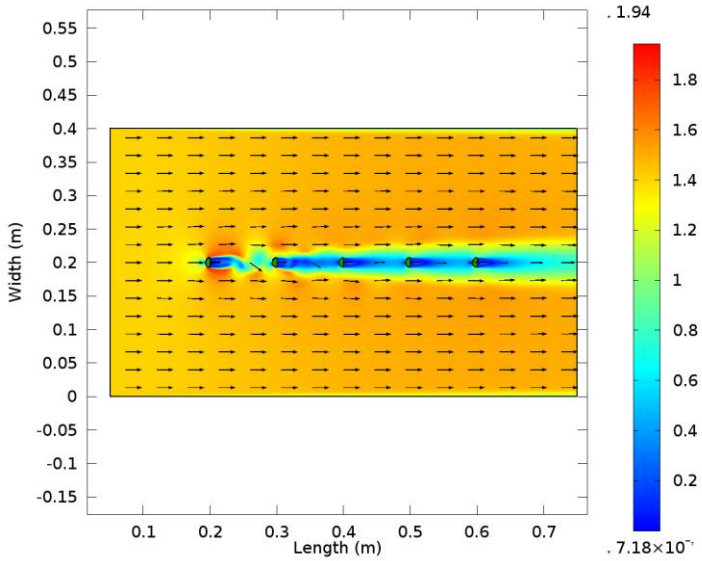

Figure 3.20. Finite element simulation for velocity distribution of multiple cantilevers in series at distance of 0.1 m.

Since the energy harvesters connected in series having distance of produced larger head loss. So, in order to resolve this problem design dimensions were increased to: 1.2 x 0.2 m. Width is reduced to 0.2 m due to computation time constraints of COMSOL software and memory limitations. Energy harvesters were placed at a distance 0.2 m and because of increased dimensions velocity distribution was almost 1.4 m/s which is same as inlet near to the boundary of fluid domain. Figure 3.21 shows the velocity distribution in the fluid domain. This time von Karman's street was observed for all 5 energy harvesters. Head loss is reduced to 37.4 mm but still the power output produced from all 5 cantilevers is 1.2 mW which is low since the average pressure difference across the surface of cantilever was reduced to 400 Pa.

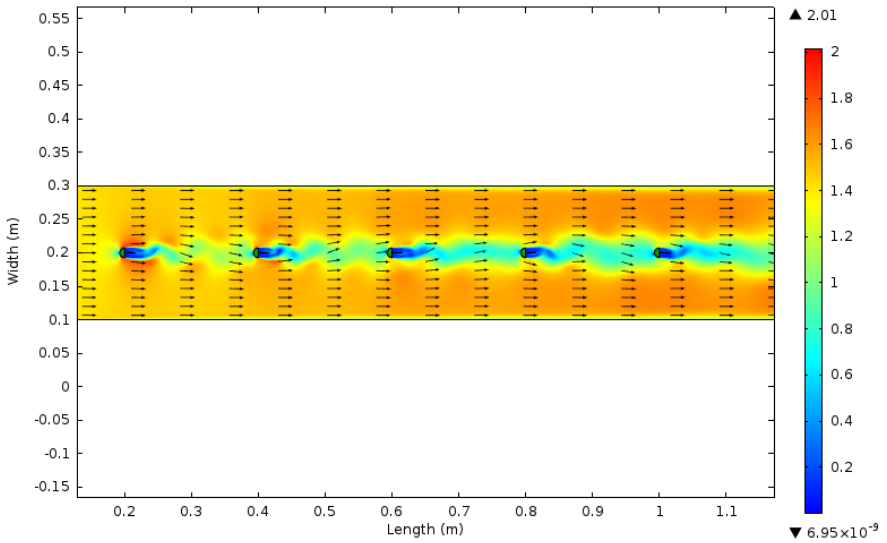

Figure 3.21. Finite element simulation for velocity distribution of multiple cantilevers in series at distance of 0.2 m.

5 energy harvesters were arranged in parallel with an equal distance of 0.1m in the fluid channel for the second analysis. The dimension of rectangular conduit is altered to: 0.4 m x 0.7 m. Automatic meshing with fluid dynamics mode is applied in this model having 27112 domain elements and 742 boundary elements as presented in Figure 3.22. The results observed in this analysis were better than 5 cantilevers in series because less velocity is disturbed which has positive impact on the pipe performance. In addition, von Karman's street is observed in all the cantilevers. Figure 3.23 demonstrates that near the rectangular fluid flow domain velocity remained 1.4 m/s. Variation of velocity from 2 m/s to 0.2 m/s is seen at the areas near the energy harvester due to bluff body presence.

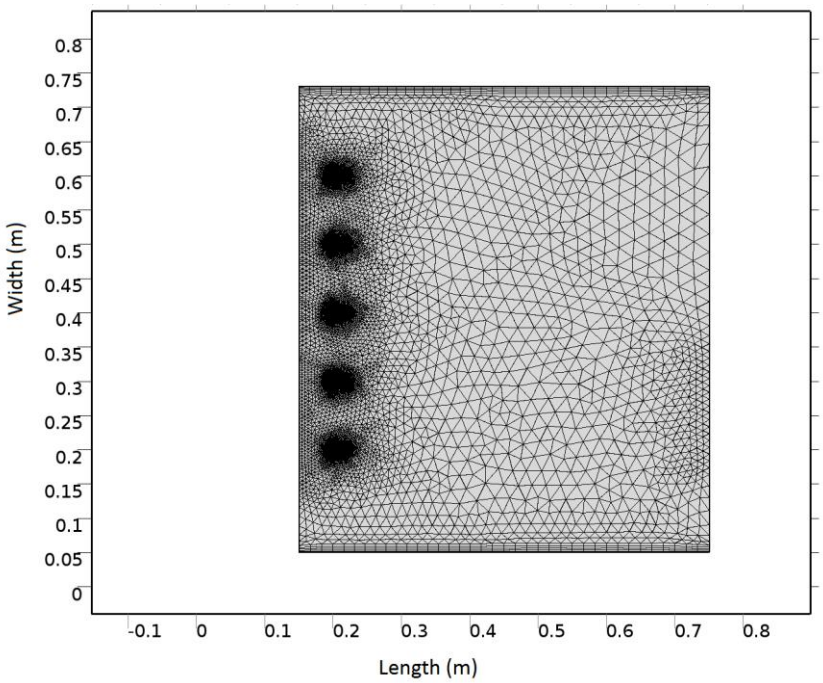

Figure 3.22. Mesh for multiple cantilevers in parallel energy harvester model.

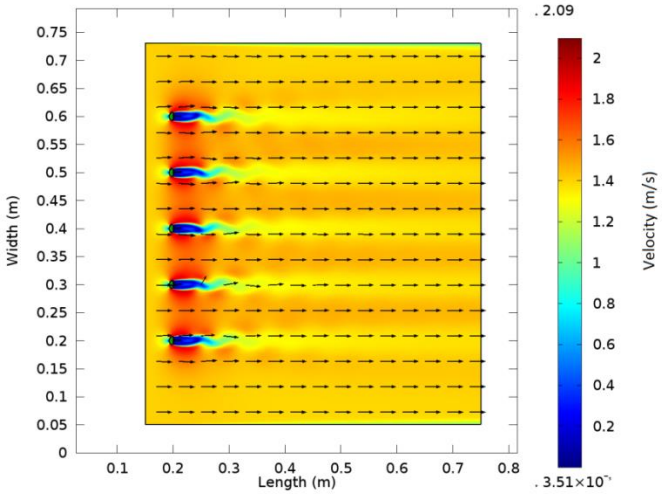

Figure 3.23. Finite Element Simulation for velocity distribution of multiple cantilevers in parallel.

3.5 Energy Requirements of In-Pipe Wireless Sensor Nodes

The processing and transmission power requirement of a wireless sensor node does not have to be instantaneously generated by the energy harvester, since the node is not expected to be continuously active. The idle time between data capture and transmissions depends on the WSN system design and associated algorithms, and may vary between many milli-seconds to minutes. Similarly, the total transmission time will depend on the number of data packets communicated, and may not last more than tens or hundreds of micro-seconds (μs). Therefore, while the power electronics design in the node has to target active power dissipation constraints, energy requirements are more relevant to the design of the energy harvester. The data packet size can be taken as 512 bytes since it is enough to meet the requirements of WSN with a data transmission and receiving rate of 4800 bits per second (bps) [2]. It means that data transmission or receiving time is 0.85 sec for the active power dissipation of the representative 2.02 W which means an energy requirement of 1.72 J. Suppose that WSN has an active power dissipation requirement every 5 minutes. An energy harvester constantly generating 0.41 mW will have generated 123 mJ in five minutes, considering 50% power conversion efficiency between generation and application. It means that there is a requirement of 15 PZT energy harvesters connected in parallel to a single bluff body to meet the energy requirements of WSN.

Energy storage device is needed for an energy harvester continuously generating energy. Traditional electrolytic capacitors, super capacitors and rechargeable batteries can be used as energy storage option for PZT energy harvester [43]. Electrolytic capacitor is not an attractive option to be used as an energy storage device for PZT

energy harvester since it has low energy density [44]. M.J. Guan et al. investigated both rechargeable batteries such as NiMH, lithium and super capacitors [45]. It is concluded in the study that leakage resistance should be high for energy storage device. In addition, it should have adaptability with power electronics circuit with enough energy capacity. Energy capacity is dependent upon charge capacity and rated voltage of energy storage device.

Table 3.5 illustrates some standard energy capacities of super capacitors and rechargeable batteries. It can be seen from the table that rechargeable batteries have much more higher density than super capacitor but still super capacitor having discharging voltage from 4V to 2V can easily meet the requirement of WSN.

Table 3.5 Different types of energy storage devices [43, 44].

Energy Storage Device	Charge Capacity	Unit	Energy Capacity (J)
Capacitor	0.47	F	7.1
NiMH Battery	110	mAh	475.2
Lithium Battery	190	mAh	2462.4

CHAPTER 4 - PERFORMANCE IMPACT ANALYSIS ON PIPE

In this chapter, a method is presented to carry out quantitative analysis of performance impact due to installation of a piezoelectric energy harvester into the Turkey-Cyprus pipeline project. The objective is to calculate the head loss and analyze how much more pressure is needed from the source to maintain the normal fluid flow.

Figure 4.1 shows the schematic model for finite element simulation with 20 points at the inlet to estimate spatial average pressure from the data extracted from these points. Zero pressure condition is used at the outlet of the simulation domain.

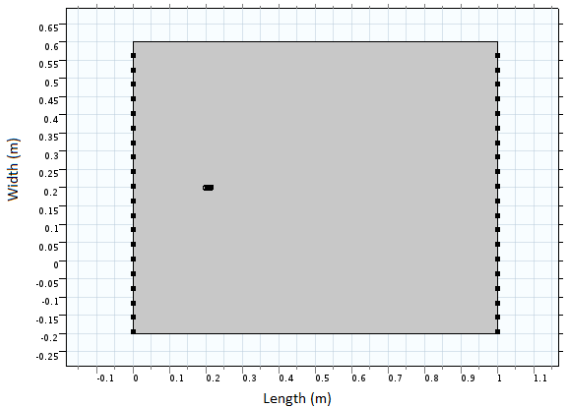

Figure 4.1. Schematic model of energy harvester having 20 points at inlet and outlet.

Bernoulli Equation is used to calculate head loss and is represented in Equation 4.1 [46].

$$\frac{p_1}{\gamma} + z_1 + \frac{v_1^{\,2}}{2g} = \frac{p_2}{\gamma} + z_2 + \frac{v_2^{\,2}}{2g} + H \qquad (4.1)$$

where g is acceleration due to gravity, z_1 is elevation from the reference point at the inlet and z_2 is the elevation of reference point at the outlet; γ is unit weight of water, p_1 and v_1 are the pressure and velocity at the inlet, p_2 and v_2 are the pressure and velocity at the outlet respectively and H shows head loss. z_1 and z_2 are equal for in this analysis since the elevation from the inlet and outlet are same. v_1 and v_2 are approximately same, g is constant so Equation 4.1 is further simplified to Equation 4.2 for the head loss calculation.

$$H = \frac{p_1 - p_2}{\gamma} \qquad (4.2)$$

Automatic physics controlled mesh with fluid dynamics mode is applied to get uniform and refined elements distribution in the model which is shown in Figure 4.2. It depicts that the mesh at the inlet and energy harvester is much finer as compared to the other fluid domain region which is the point of interest in this analysis.

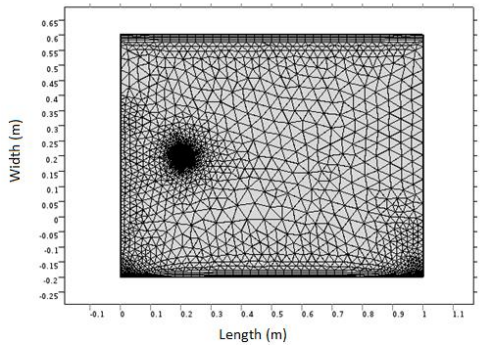

Figure 4.2. Physics controlled free tetrahedral mesh for performance impact model.

Figure 4.3 shows the finite element distribution of velocity results. According to the this figure, velocity distribution is slightly changed from 1.4 m/s to 1.2 m/s just for a small distance of 0.1 m near to the energy harvester. No change in velocity is seen for the rest of the fluid domain which shows that the impact of energy harvester is very small if installed in to the pipe. PZT cantilever in series. Spatially averaged-pressure is calculated as 30 Pa using 20 points located on the inlet. As the unit, weight of water is 9807 N/m^3, the total head loss is found to be approximately 3 mm. Head loss of 1.5 mm is found from finite element results without an energy harvester. The head loss increased to 3 mm when a PZT energy harvester is added to fluid domain which means an extra head loss of 1.5 mm, is introduced.

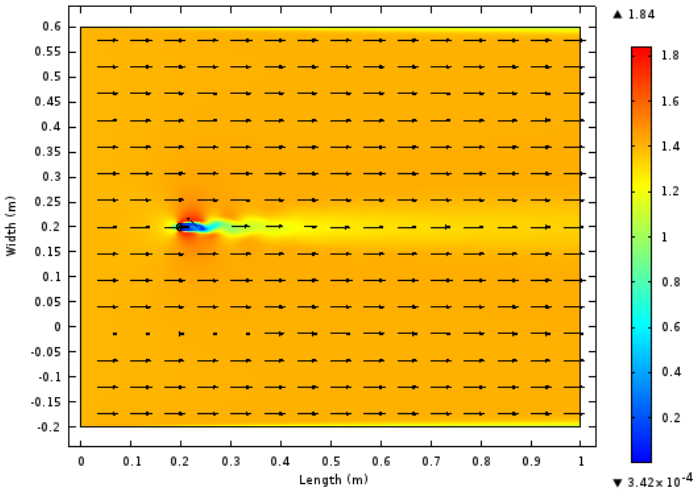

Figure 4.3. Finite element simulation results for in-pipe velocity distribution.

All possible combination of energy harvesters are compared with respect to head loss and power output in Table 4.1. It can be seen from the table that parallel arrangement of energy harvesters having D-shaped bluff body is capable to produce maximum power output of 4.05 mW at the expense of only 15 mm total head loss a so it

is considered maximum power output at the expense of smaller head loss as compared to other combinations.

Table 4.1 Power Output and total head loss comparison for different arrangements of energy harvesters.

	Total head loss (mm)	**Power Produced (mW)**	
Without Energy harvester	1.5	Not Applicable	
D-shaped bluff Body PZT energy harvester (Single)	3	0.82	
I-shaped bluff body PZT energy harvester	17.2	2.25	
	5 PZT energy harvesters head loss (mm)	**Power Produced (mW)**	**Distance between energy harvesters (mm)**
D-shaped bluff Body PZT energy harvester (Series)	88.2	1.5	100
D-shaped bluff Body PZT energy harvester (Series)	37.4	1.2	200
D-shaped bluff Body PZT energy harvester (Parallel)	15	4.05	100

Chapter 5 - CONCLUSIONS AND FUTURE WORK

5.1 Conclusions

Underwater pipelines are often necessary to transport valuable resources between patches of land, and are expected to have increased utilization across the globe with the steep population increase on one hand, and unbalanced depletion of resources on the other. It is desirable to automate monitoring of various performance parameters associated with the pipelines through WSNs to ensure longevity of use and reduced running costs. However, such pipelines are not easily accessible, and are subject to harsh environments such as salt water and underwater currents. Therefore, an ideal node in this sort of network is embedded into the pipeline, and does not require batteries with regular replacement provisions. Using an energy harvester as the power source becomes a desirable option. A method for near-optimal energy harvester module design is presented in this research to enable a self-powered wireless sensor node for in-pipe monitoring using kinetic energy of water flow. A piezoelectric bimorph cantilever is proposed to be the most suitable option because of its low maintenance and minimum impact. A crude analytical model provides a starting point for the design, which is tuned through finite element modeling and simulation. Recently constructed Turkey-Cyprus water pipeline project is taken as a case study for this research.

The power output results for the optimized geometry is verified using analytical calculations and finite element simulations. In addition, comparative analysis is carried

out for PZT energy harvester attached to D-shaped and I-shaped bluff bodies to determine which one of them is more feasible to install in pipelines. For this purpose, important parameters including electrical power output and performance impact on the pipe are compared and analyzed in detail. In addition, finite element simulations are done for the validation of analytical results which is one of the most important parts of this research. The results show that with an average water velocity of 1.4 m/s, the designed energy harvester is scalable to produce power between 820 μW (single) to 12.3 mW (15 in parallel) with a negligible impact of 3.88 mm head loss. In a WSN system with high data transmission distance and power demand, it is possible to iterate on the methodology described in this work to scale the 1-dimensional array presented here to 2-dimensional array of cantilevers at the cross-section of the pipe for more power generation.

In this study, detailed finite element model of turbine is not investigated and power conversion interface implementation circuit detailed analysis is not done. In addition, finite element simulation of different energy harvesters connected to a single bluff body is not performed. The scope of this study is limited to the near optimal design method with minimum impact on the pipe performance where two types of bluff bodies are used for comparison. This study can be expanded by adding more shapes of bluff bodies which may further improve the results of this research. The comprehensive analysis shows that it is possible to install energy harvester having the capability to produce electrical energy to meet the power requirements of the WSN to monitor the Turkey-Cyprus Water pipeline project.

5.2 Future Work

According to [35], different energy harvesters can be placed at equal distance in parallel to each other attached to a single bluff body as shown in Figure 5.1 with sufficient spacing to have zero lateral interaction, since the width of the pipe is 1.6 m. With the width of each cantilever set as 7.142 mm, a wide horizontal spacing of 71.42 mm (10x the cantilever width) and additional spacing on the sides would allow up to 20 energy harvester cantilevers in a row. An arrangement of this nature would be able to produce more than sufficient energy to support various WSN systems.

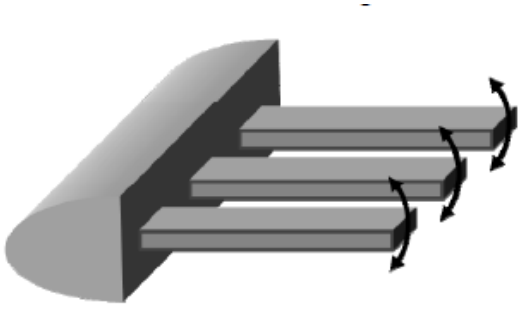

Figure 5.1. Schematic diagram of cantilevers beside each other [35].

According to [15], these can be organized to a three dimensional system in various junctures. As shown in Figure 5.2, multiple PZT cantilevers are connected to a single bluff body. In next step, multiple arrangements of cantilevers connected to a single bluff body are arranged in series to form a 2D unit. Parallel arrangement of these 2D units formed a 3D matrix of energy harvesters to generate large amount of power for the wireless sensor network.

This study can be expanded to 3D finite element simulations where multiple energy harvesters can be deployed on a single bluff body, and then performance impact of those multiple cantilevers can be analyzed in detail. In addition, we need to do performance impact on the pipe for installing hundreds and thousands of energy harvesters so experimental or computational study is required for this purpose to calculate the total head loss if we deploy energy harvesters by using this method. Another area of potential research involves identifying methods to optimize the total number of harvesters from one end to the other end of a given pipe to support a full WSN, which relates to algorithms needed to optimize the WSN size and form for in-pipe monitoring.

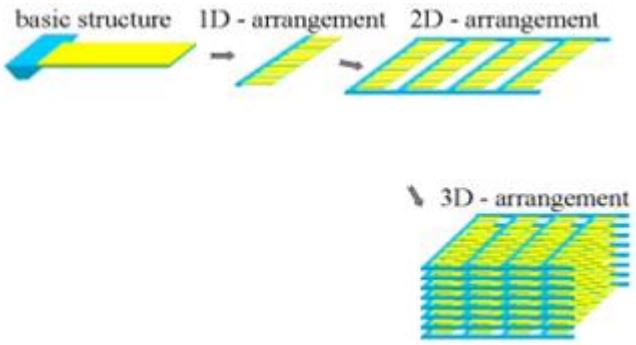

Figure 5.2. Schematic diagram of energy harvester arrangement to create useful power [15].

REFERENCES

[1] N. Mohamed, I. Jawhar, J. Al-Jaroodi, and L. Zhang, “Monitoring Underwater PIpelines Using Sensor Networks,” in *2010 12th IEEE International Conference on High Performance Computing and Communications (HPCC)*, 2010, pp. 346–353.

[2] N. Mohamed, I. Jawhar, J. Al-Jaroodi, and L. Zhang, “Sensor Network Architectures for Monitoring Underwater Pipelines,” *Sensors*, vol. 11, no. 11, pp. 10738–10764, Nov. 2011.

[3] M. I. Mohamed, W. Y. Wu, and M. Moniri, “Power harvesting for smart sensor networks in monitoring water distribution system,” in *2011 IEEE International Conference on Networking, Sensing and Control (ICNSC)*, 2011, pp. 393–398.

[4] I. F. Akyildiz, W. Su, Y. Sankarasubramaniam, and E. Cayirci, “Wireless sensor networks: a survey,” *Comput. Netw.*, vol. 38, no. 4, pp. 393–422, Mar. 2002.

[5] L. Mateu, M. Echeto, and F. de Borja, “Review of energy harvesting techniques and applications for microelectronics,” 2005.

[6] V. Raghunathan, A. Kansal, J. Hsu, J. Friedman, and M. Srivastava, “Design considerations for solar energy harvesting wireless embedded systems,” in *IPSN 2005. Fourth International Symposium on Information Processing in Sensor Networks, 2005.*, 2005, pp. 457–462.

[7] B. Ozerdem and H. M. Turkeli, “Wind energy potential estimation and micrositting on Izmir Institute of Technology Campus, Turkey,” *Renew. Energy*, vol. 30, no. 10, pp. 1623–1633, Aug. 2005.

[8] “Turbines | Francis | Pelton | Propeller | Hydro-Québec.” [Online]. Available: http://www.hydroquebec.com/learning/hydroelectricite/types-turbines.html. [Accessed: 04-Jun-2016].

[9] G. Ye and K. Soga, “Energy Harvesting from Water Distribution Systems,” *J. Energy Eng.*, vol. 138, no. 1, pp. 7–17, 2012.

[10] J. A. R. Azevedo and F. E. S. Santos, “Energy harvesting from wind and water for autonomous wireless sensor nodes,” *IET Circuits Devices Syst.*, vol. 6, no. 6, pp. 413–420, Nov. 2012.

[11] T. H. Ching, T. Ibrahim, F. I. A. Aziz, and N. M. Nor, “Renewable energy from UTP water supply,” in *2011 International Conference on Electrical, Control and Computer Engineering (INECCE)*, 2011, pp. 142–147.

[12] J. Chen, H. X. Yang, C. P. Liu, C. H. Lau, and M. Lo, “A novel vertical axis water turbine for power generation from water pipelines,” *Energy*, vol. 54, pp. 184–193, Jun. 2013.

[13] “Lucid Energy | LucidPipe™ Power System.” [Online]. Available: http://www.lucidenergy.com/lucid-pipe/. [Accessed: 24-Jun-2016].

[14] M. S. Bhuyan, B. Y. Majlis, M. Othman, S. H. M. Ali, C. Kalaivani, and S. Islam, “Development of a Fluid Actuated Piezoelectric Micro Energy Harvester: Finite

Element Modeling Simulation and Analysis," *Asian J. Sci. Res.*, vol. 6, no. 4, pp. 691–702, Apr. 2013.

[15] S. Pobering and N. Schwesinger, "A Novel Hydropower Harvesting Device," in *2004 International Conference on MEMS, NANO and Smart Systems, 2004. ICMENS 2004. Proceedings*, 2004, pp. 480–485.

[16] H. D. Akaydin, N. Elvin, and Y. Andreopoulos, "Energy Harvesting from Highly Unsteady Fluid Flows using Piezoelectric Materials," *J. Intell. Mater. Syst. Struct.*, Mar. 2010.

[17] S. Sudevalayam and P. Kulkarni, "Energy Harvesting Sensor Nodes: Survey and Implications," *IEEE Commun. Surv. Tutor.*, vol. 13, no. 3, pp. 443–461, Third 2011.

[18] "Wiley: Protocols and Architectures for Wireless Sensor Networks - Holger Karl, Andreas Willig." [Online]. Available: http://eu.wiley.com/WileyCDA/WileyTitle/productCd-0470095105.html. [Accessed: 24-Jun-2016].

[19] A. Kansal, J. Hsu, S. Zahedi, and M. B. Srivastava, "Power Management in Energy Harvesting Sensor Networks," *ACM Trans Embed Comput Syst*, vol. 6, no. 4, Sep. 2007.

[20] M. K. Stoj¿ev, M. R. Kosanovi¿, and L. R. Golubovi¿, "Power management and energy harvesting techniques for wireless sensor nodes," in *9th International Conference on Telecommunication in Modern Satellite, Cable, and Broadcasting Services, 2009. TELSIKS '09*, 2009, pp. 65–72.

[21] B. Benson, Y. Li, R. Kastner, B. Faunce, K. Domond, D. Kimball, and C. Schurgers, “Design of a low-cost, underwater acoustic modem for short-range sensor networks,” in *OCEANS 2010 IEEE - Sydney*, 2010, pp. 1–9.

[22] “Products / Underwater Acoustic Modems / Underwater Acoustic Modems | EvoLogics GmbH.” [Online]. Available: https://www.evologics.de/en/products/acoustics/index.html. [Accessed: 24-Jun-2016].

[23] “Acoustic Modems Archives,” *Desert Star Systems LLC.* .

[24] “AquaComm: Underwater Wireless Modem.” [Online]. Available: http://www.dspcomm.com/products_aquacomm.html. [Accessed: 24-Jun-2016].

[25] L. B. Hörmann, P. M. Glatz, C. Steger, and R. Weiss, “A wireless sensor node for river monitoring using MSP430 #x00AE; and energy harvesting,” in *Education and Research Conference (EDERC), 2010 4th European*, 2010, pp. 140–144.

[26] “Signet Measurement and Control - GF Piping Systems.” [Online]. Available: http://www.gfps.com/country_US/en_US/products/sensors.html. [Accessed: 24-Jun-2016].

[27] “MS5541C—Pressure Sensors–Digital-High Level Analog Pressure Sensor Modules–Measurement Specialties.” [Online]. Available: http://www.meas-spec.com/product/t_product.aspx?id=5035. [Accessed: 24-Jun-2016].

[28] “Water Pipeline from Turkey to Cyprus—1,600 mm Diameter Polyethylene 100 Pipeline and Its Flange-Technology Solution - 9780784479360.018.” [Online].

Available: http://ascelibrary.org/doi/pdf/10.1061/9780784479360.018. [Accessed: 24-Jun-2016].

[29] "Seamap » Ampair UW100™." .

[30] D. Hoffmann, A. Willmann, R. Göpfert, P. Becker, B. Folkmer, and Y. Manoli, "Energy Harvesting from Fluid Flow in Water Pipelines for Smart Metering Applications," *J. Phys. Conf. Ser.*, vol. 476, p. 12104, Dec. 2013.

[31] "Datasheet_MT_20080408.FH10 - Datasheet_MT_ENG[1].pdf." [Online]. Available: http://www.solarlink.de/PDF-Files/Phocos/Wasserturbine/Datasheet_MT_ENG%5B1%5D.pdf. [Accessed: 25-Jun-2016].

[32] S. Pobering, S. Ebermeyer, and N. Schwesinger, "Generation of electrical energy using short piezoelectric cantilevers in flowing media," 2009, vol. 7288, pp. 728807-728807–8.

[33] S. Pobering and N. Schwesinger, "Power supply for wireless sensor systems," in *2008 IEEE Sensors*, 2008, pp. 685–688.

[34] "PIEZOELECTRIC ENERGY HARVERSTER USING FLOW-INDUCED VIBRATION." [Online]. Available: http://cap.ee.ic.ac.uk/~pdm97/powermems/2008/pdfs/197-200%20Kim,%20K.H.pdf. [Accessed: 25-Jun-2016].

[35] E. Bischur, S. Pobering, M. Menacher, and N. Schwesinger, "Piezoelectric energy harvester operating in flowing water," 2010, vol. 7643, p. 76432Z–76432Z–8.

[36] “THE DESIGN OF VORTEX INDUCED VIBRATION FLUID KINETI C ENERGY HARVESTERS.” [Online]. Available: http://cap.ee.ic.ac.uk/~pdm97/powermems/2012/poster/P-002.pdf. [Accessed: 25-Jun-2016].

[37] H. Li, C. Tian, and Z. D. Deng, “Energy harvesting from low frequency applications using piezoelectric materials,” *Appl. Phys. Rev.*, vol. 1, no. 4, p. 41301, Dec. 2014.

[38] J. Qiu, H. Jiang, H. Ji, and K. Zhu, “Comparison between four piezoelectric energy harvesting circuits,” *Front. Mech. Eng. China*, vol. 4, no. 2, pp. 153–159, Mar. 2009.

[39] G. K. Ottman, H. F. Hofmann, A. C. Bhatt, and G. A. Lesieutre, “Adaptive piezoelectric energy harvesting circuit for wireless remote power supply,” *IEEE Trans. Power Electron.*, vol. 17, no. 5, pp. 669–676, Sep. 2002.

[40] E. Lefeuvre, D. Audigier, C. Richard, and D. Guyomar, “Buck-Boost Converter for Sensorless Power Optimization of Piezoelectric Energy Harvester,” *IEEE Trans. Power Electron.*, vol. 22, no. 5, pp. 2018–2025, Sep. 2007.

[41] J. Zhao and Z. You, “A shoe-embedded piezoelectric energy harvester for wearable sensors,” *Sensors*, vol. 14, no. 7, pp. 12497–12510, 2014.

[42] “Meshing your Geometry: When to Use the Various Element Types,” *COMSOL Blog*, 04-Nov-2013. .

[43] H. A. Sodano, D. J. Inman, and G. Park, “Generation and Storage of Electricity from Power Harvesting Devices,” *J. Intell. Mater. Syst. Struct.*, vol. 16, no. 1, pp. 67–75, Jan. 2005.

[44] M. J. Guan and W. H. Liao, “On the efficiencies of piezoelectric energy harvesting circuits towards storage device voltages,” *Smart Mater. Struct.*, vol. 16, no. 2, p. 498, 2007.

[45] M. J. Guan and W. H. Liao, “Characteristics of Energy Storage Devices in Piezoelectric Energy Harvesting Systems,” *J. Intell. Mater. Syst. Struct.*, vol. 19, no. 6, pp. 671–680, Jun. 2008.

[46] J. A. Schetz and A. E. Fuhs, *Fundamentals of Fluid Mechanics*. John Wiley & Sons, 1999.

Appendix A

Conference Proceeding I:

Authors: Fassahat Ullah Qureshi, Ali Muhtaroglu, Kagan Tuncay

Conference Name: 5th International Conference on Energy Aware Computing & Applications (ICEAC 2015)

Cairo, Egypt

Title: A Method to Integrate Energy Harvesters into Wireless Sensor Nodes for Embedded In-Pipe Monitoring Applications

URL: http://ieeexplore.ieee.org/stamp/stamp.jsp?arnumber=7352196

Conference Proceeding II:

Authors: Fassahat Ullah Qureshi, Ali Muhtaroglu, Kagan Tuncay

Conference Name: 4th European Conference on Renewable Energy Systems, Istanbul, TURKEY, 28-31 August 2016)

Title: Sensitivity Analysis to design near optimal piezoelectric energy harvester to produce power for Wireless Sensor Nodes for underwater pipelines monitoring applications (Full Paper Accepted)

Conference Proceeding III:

Authors: Fassahat Ullah Qureshi, Ali Muhtaroglu, Kagan Tuncay

Conference Name: 4th European Conference on Renewable Energy Systems, Istanbul, TURKEY, 28-31 August 2016)

Title: Comparative Analysis between D Shaped and I Shaped bluff body for piezoelectric energy harvesting to power Wireless Sensor Nodes for pipeline monitoring applications (Full Paper Accepted)